SKB

TECHNICAL REPORT 93-03

MX 80 clay exposed to high temperatures and gamma radiation

R Pusch[1], O Karnland[1], A Lajudie[2], A Decarreau[3]

[1] Clay Technology AB, Sweden
[2] CEA, France
[3] Univ. de Poitiers, France

December 1992

SVENSK KÄRNBRÄNSLEHANTERING AB
SWEDISH NUCLEAR FUEL AND WASTE MANAGEMENT CO
BOX 5864 S-102 48 STOCKHOLM
TEL. 08-665 28 00 TELEX 13108 SKB S
TELEFAX 08-661 57 19

MX 80 CLAY EXPOSED TO HIGH TEMPERATURES AND GAMMA RADIATION

R Pusch[1], O Karnland[1], A Lajudie[2], A Decarreau[3]

1 Clay Technology AB, Sweden
2 CEA, France
3 Univ. de Poitiers, France

December 1992

FINAL REPORT ON SKB/CEA

MX 80 CLAY EXPOSED TO HIGH TEMPERATURES AND GAMMA RADIATION

December 1992

CLAY TECHNOLOGY AB

R. PUSCH
O. KARNLAND

CEA

A. LAJUDIE

UNIV. DE POITIERS

A. DECARREAU

ABSTRACT (ENGLISH)

MX-80 bentonite saturated with pressurized weakly brackish water, was heated up to 130°C with and without γ-radiation for 1 year. The smectite content remained largely intact while accessory minerals like feldspars were strongly affected. The hydraulic conductivity was not altered but slight cementation by precipitated silica took place.

ABSTRACT (SWEDISH)

MX-80 bentonit mättad med trycksatt, svagt bräckt vatten, värmdes upp till 130°C med och utan γ-strålning under 1 år. Smektitinnehållet förblev i stort sett opåverkat medan accessoriska mineral såsom fältspat påverkades starkt. Hydrauliska konduktiviteten ändrades inte men viss cementering ägde rum genom utfällning av kiselföreningar.

TABLE OF CONTENTS

SUMMARY

MX-80 clay, saturated with very weakly brackish Allard water, was heated up to 130°C under hydrothermal conditions with and without γ-radiation for 1 year. Chemical and mineralogical analyses as well as physical testing showed that no major changes in smectite content had taken place in the test period. A major conclusion is that the hydraulic conductivity was not changed, while the rheological properties including expandability were slightly altered. Microstructural changes in the form of precipitations were obvious in the part that had been heated to 130°C and which had also become significantly stiffer.

The major mineralogical alterations were the disappearance of feldspars and formation of sulphates; the montmorillonite appearing to be largely unaffected except for slight dissolution and transformation to 10 Å minerals and possibly pseudo-chlorite. Rather insignificant interaction had taken place between the clay and the steel heater despite the rather extensive corrosion of the steel heater but iron had diffused to about 10 mm depth in the clay.

The overall conclusions are that the combined effect of strong γ radiation and heating up to 130°C under repository-like conditions with electrolyte-poor porewater in the clay causes only insignificant alteration of the smectite content and physical properties. The most important effect on the latter is slight cementation by precipitation of released silica.

1 PURPOSE AND OUTLINE OF THE TEST

The major idea with the test was to expose a 7 cm long water saturated sample of MX-80 bentonite clay to a constant temperature gradient of 40°C (Max. T=130°C and min. T=90°C) with and without applying strong γ radiation, for simulating the conditions in a repository. The test was conducted at CEA:s laboratories at Saclay close to Paris and ran for 1 year. Detailed analyses of the mineralogical and chemical changes were then performed both at CEA and at Clay Technology AB, Sweden. The physical properties before and after treatment were determined by Clay Technology AB.

MX-80 clay saturated with Allard water, i.e. very weakly brackish water with sodium as major cation, was confined in a cylindrical chamber with one end closed by steel that was exposed to 130°C without γ radiation in one experiment and with γ radiation in a preceding experiment. The other end consisted of a filter connected to a vessel with Allard water that was pressurized to 1.5 MPa throughout the tests, such that the physical conditions under the hydrothermal experiments were well defined.

After termination of the tests, the samples were sectioned and stored under nitrogen gas until laboratory testing took place. Detailed interim reports on specific subjects have been worked out in the course of the tests. The present document is the final report of the study.

2 METHODS FOR CLAY CHARACTERIZATION

2.1 MINERALOGY AND CHEMISTRY

2.1.1 General

Three cores of compacted MX-80 clay were prepared and analyzed as follows:

* Sample REF (Reference clay) investigated immediately after preparation
* Sample IR (Irradiated clay) exposed to 90/130°C temperature gradient and γ radiation for 1 year
* Sample non-IR (Non-irradiated clay) exposed to 90/130°C tempera- ture gradient for 1 year

2.1.2 Analaytical methods (CEA)

2.1.2.1 XRD

Physical and chemical investigations were performed on bulk specimens as well as on the minus 2μm material, i.e. the clay fraction.

For the bulk analyses the samples were gently crushed in an agate mortar under air-dry conditions. The clay fraction was separated by decanting from powdered bulk material dispersed in water. Dehydration was made by heating to 60°C.

XRD patterns were obtained by use of a Philips PW 1730 diffractometer with Fe-filtered Co$_{K\alpha}$ radiation (λ=1.789 Å). A proportional detector was used either with a continuous scanning goniometer and graphical recording, or with a step mode scanning goniometer and digital recording.

Powder patterns were obtained for the bulk samples, while the clay fraction was investigated by using oriented aggregates evaporated on glass slides. The following preparation modes were applied: 1) Ca-saturation, followed by air-drying and treatment with ethylene glycol (EG); 2) Ca-saturation, K-exchange and 2 hours heating to 300°C, followed by EG treatment. K-exchanged samples were used for estimating the proportion of high-charge to low-charge smectite: after K-saturation high-charge layers collapse while low-charge smectite maintain their expandability on EG treatment.

2.1.2.2 Chemical analyses (CEA)

Ordinary chemical analyses were made by atomic absorption spectroscopy (AAS) and flame spectroscopy using a P.E. apparatus after fusion in a $SrCl_2$ matrix.

Cation exchange capacity (CEC) was determined by saturation with ammonium acetate of the clay fraction. Exchangeable cations were determined by AAS.

FTIR spectra covering the range 4000 and 400 cm^{-1} were obtained by a Nicolet 510 equipment. 1-4 mg of the <2μm fraction pressed with 200 mg of KBr and then dehydrated at 200°C for 24 hours.

ESR spectra were recorded at 21°C in X-band (Centre de Spectroscochimie, Universite P. et M.Curie, Paris).

Mössbauer data were collected by use of an Elscint AME 30 spectrometer at room temperature, using a ^{57}Co source dispersed in an Rh-matrix (nominal strength 25 mCi).

2.1.2.3 Mineralogical analyses (Clay Technology AB)

The mineralogical analyses were intended to give a quick overall picture of major changes and were not aimed at elucidating possible transformation mechanisms.

Mineralogical characterization was made by XRD, using a Philips PW 1730 machine with CuKα radiation, with and without ethylene glycol treatment of sedimented specimens. Also, cation exchange capacity measurements were made by using strontium as exchange cation. Morphological analysis together with semi-quantitative determination of elements (EDX) was utilized for identification of precipitates.

2.1.2.4 Chemical analyses (Clay Technology AB)

The chemical analyses were intended to identify possible major changes and not to yield a detailed picture of the involved processes.

ICP spectroscopy of $LiBO_2$-melts were used for quantitative determination of SiO_2, Al_2O_3, Fe_2O_3, MnO, TiO_2, MgO, CaO, K_2O, Na_2O, and P_2O_5. The EDX electron microscopy for spot analysis and mapping gave information on major elements in discrete parts of the clay.

2.1.2.5 Microstructural analysis

Three different types of electron microscopy were applied in the present study with the following purposes:

1. Transmission electron microscopy for general characterization of microstructural features
2. Scanning EM for morphological characterization of precipitations
3. Analytical EM for qualitative and semi-quantitative element analysis

These investigations were made by use of the JEOL 200 CX STEM and Philips SEM 515 microscopes of the Dept. of Electron Microscopy, Lund University.

The preparation of specimens for transmission EM was made by freeze-drying followed by saturation with methyl/butyl acrylate, polymerization, and ultramicrotomy yielding 500-1000 Å sections (1).

Scanning EM specimens were prepared from freeze-dried samples, which were gold-coated except for the specimens used for element analysis.

2.2 PHYSICAL PROPERTIES (Clay Technology AB)

2.2.1 General

The hydraulic conductivity and the rheological properties in terms of creep behavior were investigated at Clay Technology's laboratory in Lund, Sweden.

2.2.2 Hydraulic conductivity

The specimens were transferred to a 20 mm diameter shear box in which they were exposed to slight compression by loading them to the assumed swelling pressure. Then, percolation was made with Allard water for a few days, whereafter rheological testing was conducted.

2.2.3 Rheology

A normal stress σ corresponding to the estimated swelling pressure of MX-80 clay saturated with distilled water, i.e. 6 MPa, was applied and this stress was then adjusted so that the samples expanded axially by about 10 μm in order to eliminate friction be

tween the two shear box halves. A shear stress τ corresponding to about 10 % of the shear strength of equally dense unheated MX-80 clay saturated with distilled water, i.e. 260 kPa, was applied for about two days, after which the shear stress was doubled and the creep again recorded for two days. The low stress level was selected in order not to disturb the microstructure, which was investigated subsequently.

Automatic recording of the shear displacement was made and the angular shear strain evaluated by applying the expression in Eq.1, which was derived in an earlier FEM-based identification of a suitable strain parameter from this kind of shear tests (2).

$$\gamma = \frac{3\varepsilon}{\sqrt{1 - \frac{\Sigma\Delta}{\Delta f}}} \qquad (1)$$

where Δ is the shear displacement for the respective load step and $\varepsilon = \Delta/D$, D being the diameter of the shear-box. Δf is the total shear displacement at failure.

A generalized form of the creep rate is given by Eq. 2, from which the characteristic parameters t_o and B can be derived. This is preferably made by a least square fit of recorded creep data to the expression in Eq. 3.

$$\dot{\gamma} = B\ (t + t_o)^{-1}, \qquad (2)$$

$$\gamma = B \ln (t + t_o) + A \qquad (3)$$

where t denotes elapsed time after onset of creep and A is a constant of integration. The B- and t_o-values evaluated from the experiments will be reported here and correlated with the influence of heat exposure.

In addition to the creep tests, experiments were made in which samples confined in the shear box under 6 MPa external pressure were allowed to expand on reducing this pressure to 5 MPa. This was expected to give information of possible transformation from fully expandable montmorillonite to collapsed 10 Å minerals, as well as of possible cementation effects.

3 DESCRIPTION OF THE TESTS

3.1 CLAY MATERIAL

The clay was sampled from industrially processed commercial MX-80 (Wyoming bentonite), which is known to be rich in montmorillonite with sodium as major adsorbed cation.

Samples for exposure to heat and radiation were prepared by compacting air-dry powder in swelling pressure oedometers and saturating them with Allard water to almost complete saturation. The samples were cylindrical with 20 mm diameter and 70 mm length; their dry density was 1.65 g/cm^3 and the water content about 23 %. The theoretical bulk density at complete water saturation was 2.05 g/cm^3.

3.2 WATER SOLUTION

The type of water which had been used for saturation of the clay and with which it was contacted throughout the test was low-electrolyte Allard water with the following composition:

Component	mmole/liter
HCO_3^-	2.014
H_4SiO_4	0.205
SO_4^{2-}	0.100
Cl^-	1.973
Ca^{2+}	0.448
Mg^{2+}	0.177
K^+	0.100
Na^+	2.836
pH	8.0-8.2

3.3 STEEL

A 5 mm thick plane disc of XC10 steel was placed in contact with one of the ends of the sample, the steel being exposed to the highest temperature (130°C) and to irradiation. At the other end, the sample contacted a sintered porous filter of acid-proof, stainless steel.

The steel at the hot, irradiated end had the following composition:

Element	%
C	0.120
Mn	0.470
Si	0.250
S	0.003
P	0.026

3.4 IRRADIATION PARAMETERS

The irradiation lasted for almost exactly 1 year, i.e. from April 1 1988 to April 3 1989, by exposing the high temperature end of the sample to γ radiation from a ^{60}Co radiation source in the Poseidon irradiator (CEN Saclay).

5 sensors were inserted in the sample for recording the dose rate along the sample, the values being:

Distance from irradiated contact, mm	Adsorbed dose rate Gy/h
0.0	3972
23.5	843
36.6	670
46.0	561
64.1	456

The total absorbed dose integrated over the sample was 3.27×10^7 Gy.

3.5 SAMPLE CHAMBER

The sample was placed in a cylindrical chamber with the steel plate and filter at opposite ends. The chamber had lead-throughs for the radiation gauges and for tubings used for maintaining the water pressure at 1.5 MPa (+/-0.1 MPa), as well as for heating coils by which the temperature was maintained at 130° at the irradiated end and 90° at the opposite one, and for gauges through which the temperature were recorded in the sample (Fig.3-1).

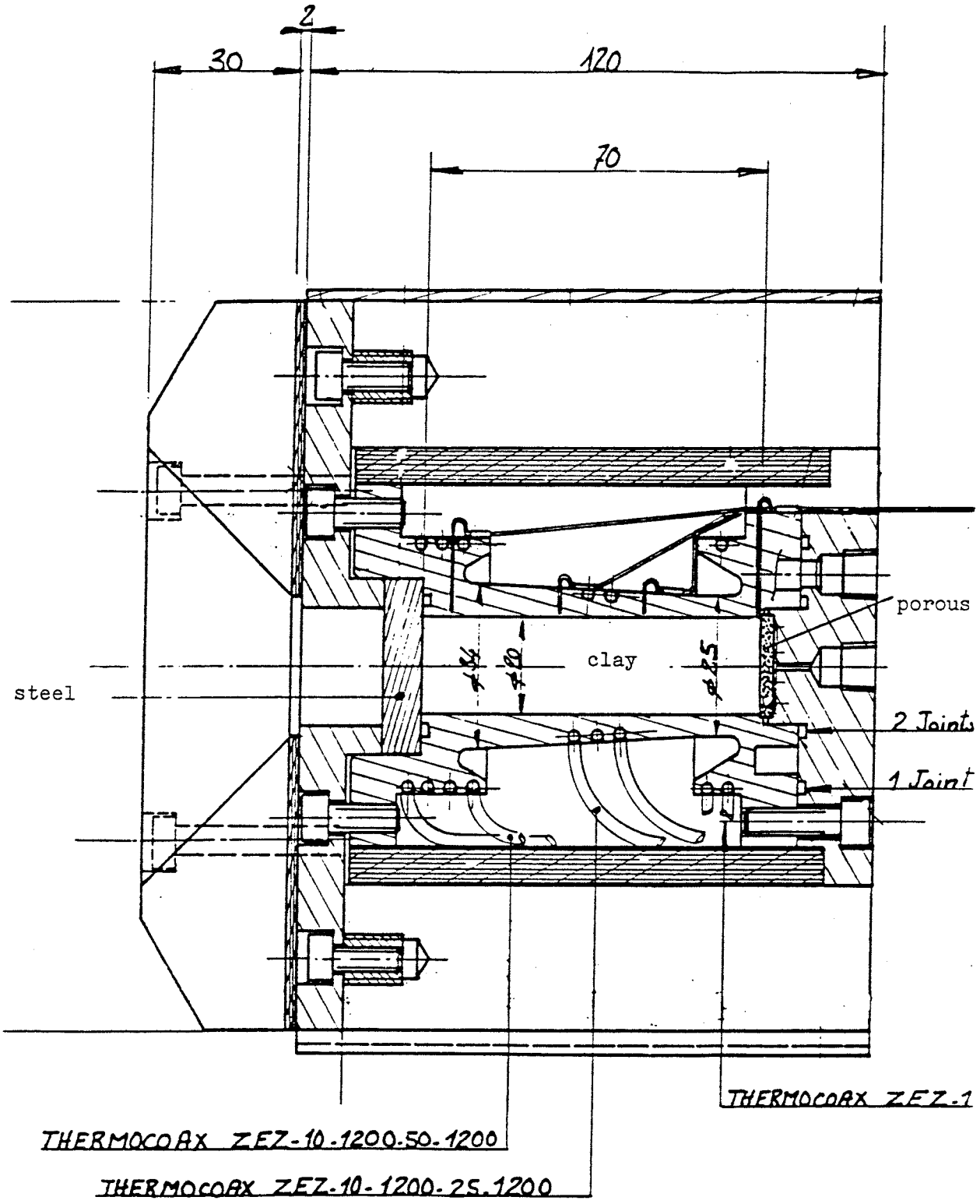

Figure 3-1 Chamber with the clay sample confined for the heating and irradiation experiment (CEA)

4 TEST RESULTS

4.1 SAMPLING

Figs.4-1 and 4-2 show the sectioning principle for obtaining specimens. It was made in nitrogen gas atmosphere and resulted in 8 discs of the irradiated sample and 4 of the non-irradiated one. The irradiated disc samples were sectioned and used for analyses by CEA and Clay Technology AB, respectively.

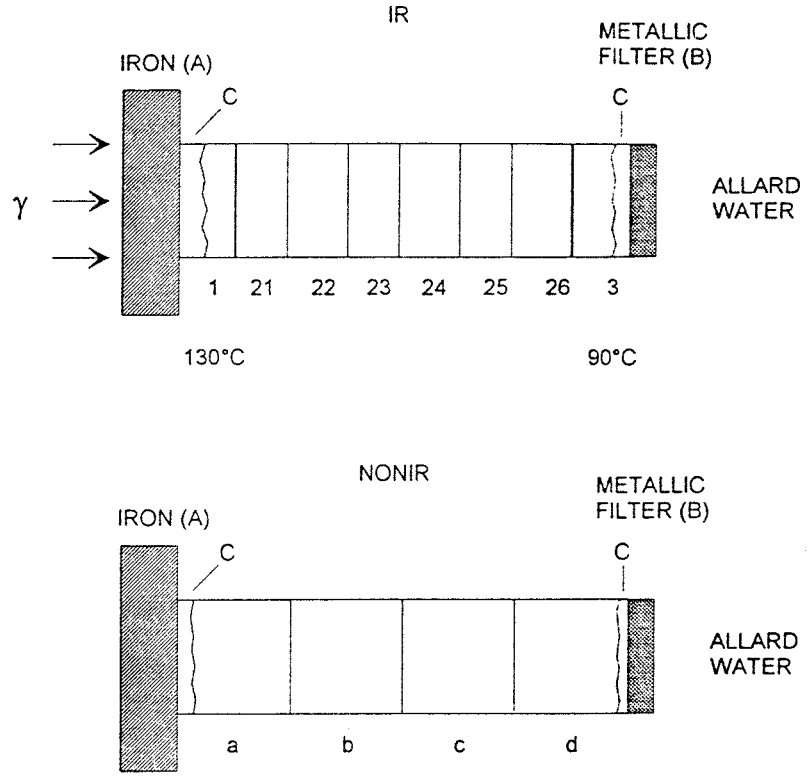

Figure 4-1 Code numbers of CEA-investigated samples. Upper: Irradiated sample. Lower: non-irradiated sample

Fig.4-2 shows the code numbering of the samples investigated by Clay Technology AB and Table 4-1 gives the approximate temperatures to which these samples had been exposed.

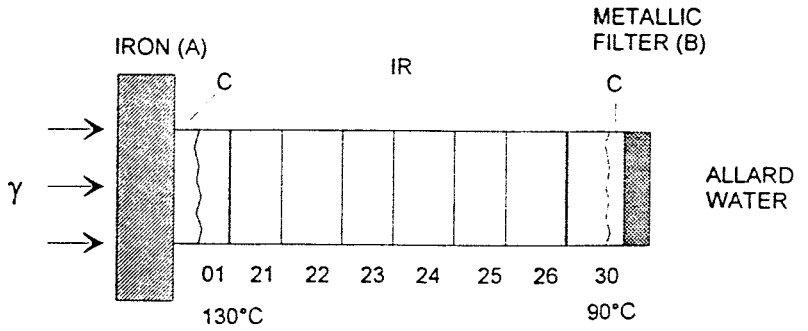

Figure 4-2 Samples investigated by Clay Technology AB

Table 4-1 Sample codes and type of analyses in Clay Technology's study: M is mineralogy, C chemistry, Mi microstructure, k hydraulic conductivity, R rheology,

Code no	Temperature	Analyses				
		M	C	Mi*	k	R
00	Reference	x	x	x	x	x
01	130°C	x	x	x	x	x
22	115°C	x	x	x	x	x
26	95°C	x	x	x	x	x

* Including EDX

4.2 MINERALOGY

4.2.1 CEA study

All the cores had remained coherent and ductile and could be sectioned without difficulty. The REF sample appeared to be somewhat heterogeneous with millimeter-sized light zones that turned out to be feldspars and calcite. The IR and NON-IR samples gave a more homogeneous impression with a somewhat darker greyish color except for the ends, which were orange-yellow to rusty in color. In the IR sample the colored zones extended up to 5 mm from the irradiated steel and to 2 mm from the filter. The NON-IR sample had colored zones that were only 1 mm thick.

4.2.1.1 XRD

REF sample

The REF sample showed spectra with the following major reflections (Fig.4-3):

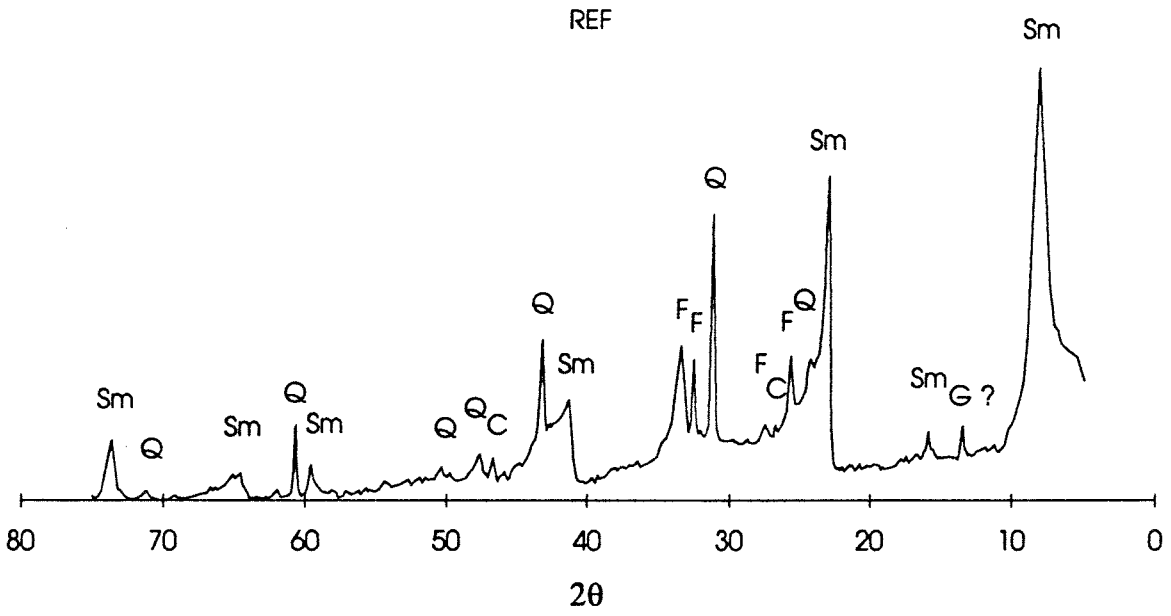

Figure 4-3 Diffraction pattern of the REF sample (bulk, packed)

* **Smectite** /(001):12.8 Å, (02-11):4.43 Å, (13-20):2.55 Å, (15-24-31):1.69 Å, (06-33):1.49 Å. The last value indicates that the smectite is dioctahedral/;

* **Quartz** /(100):4.22 Å, (101):3.33 Å, (112):1.80 Å/;

* **Na-Ca Feldspars** /(001):6.33 Å, (201):4.02 Å and others near 3.75, 3.20, 3.10 Å/;

* **Calcite** in low concentrations /(102):3.86 Å (104):3.03 Å and (110):2.49 Å/;

* **Opal** probably present in low concentrations /broad reflections at (101):4.02 Å and (200):2.49 Å/;

* **Unknown species** with reflections at 7.45 Å

IR sample

The IR sample showed characteristic reflections of smectite, quartz and feldspars but signals indicating calcite were not present (Fig.4-4). A weak reflection of anhydrite (3.46 Å) appeared in IR-3 while there

were no signs of gypsum. A small amount of hematite was also observed /(104):2.70 Å, (110):2.52 Å and (116):1.70 Å/ and of hydrous mica (illite) as well /(001):10 Å/.

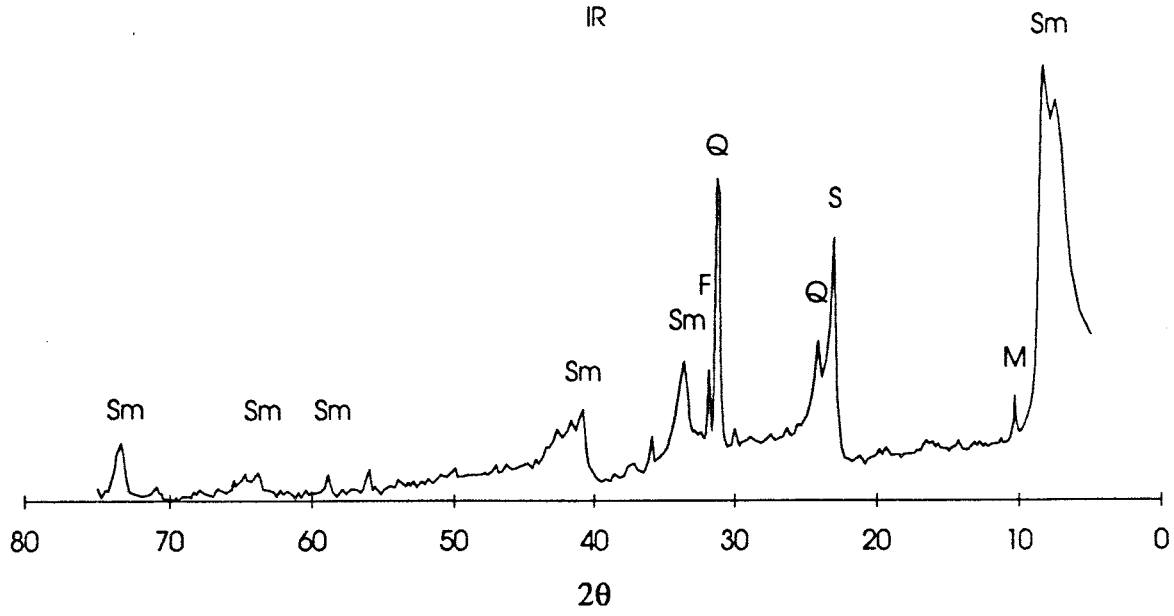

Figure 4-4 Diffraction pattern of IR sample (bulk, packed)

The amounts of quartz, feldspar and illite varied irregularly along the core which suggests a variation in the composition of the MX-80 ED material investigated.

In the IR sample only the more intense reflections of quartz and feldspar were recognized and they appeared to be broader than in the REF sample. These two minerals are concluded to have been partly dissolved in the irradiated sample.

The basal reflections (001) of the smectite in the IR sample show two maxima, i.e. at 12-13 and 14-15.5 Å, indicating that some stacks held one and others two hydrate layers, a matter that can be due to Na or Ca dominance in certain interlamellar positions and to varying humidity at the testing.

The position and shape of the other smectite reflections were not different in the IR sample than in the REF sample, indicating that the dioctahedral nature of the smectite was preserved and that crystal growth or dissolution were insignificant.

NONIR sample

The following minerals could be identified (Fig.4-5):

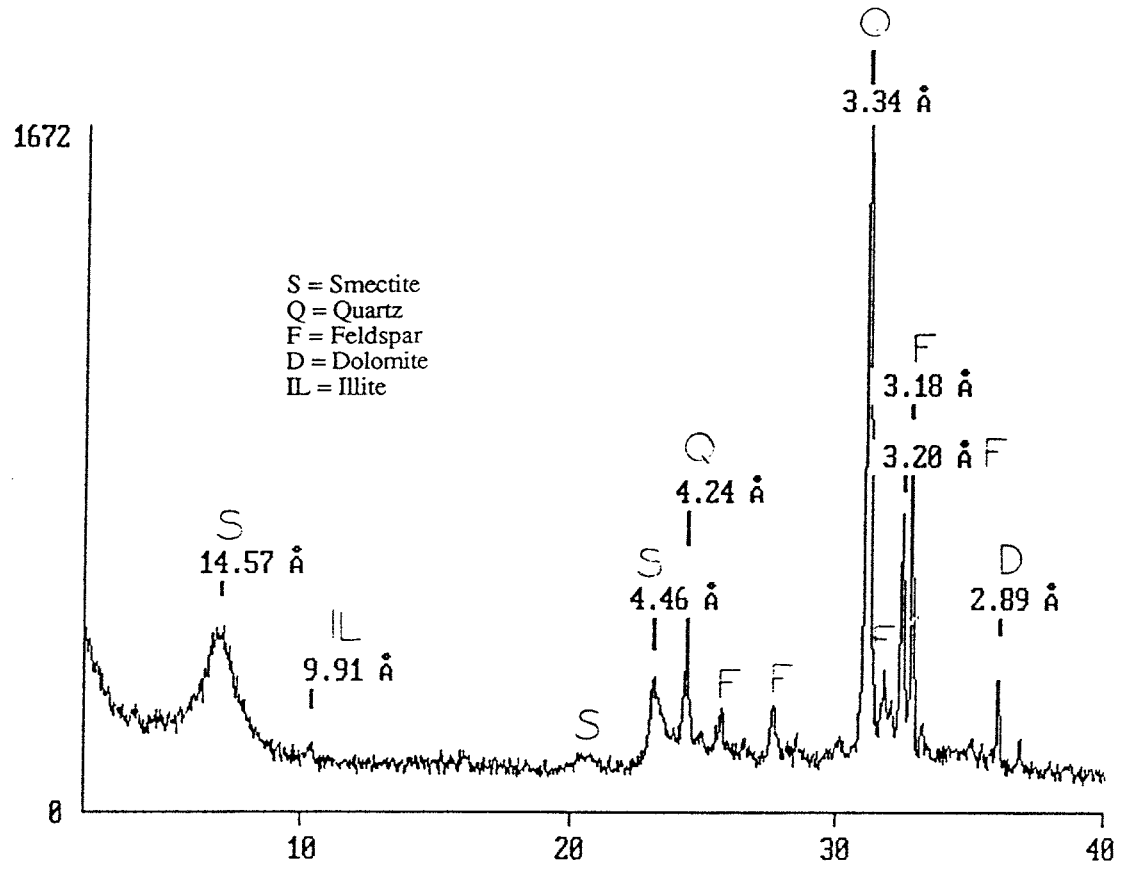

Figure 4-5 Diffraction pattern of NONIR sample (bulk, packed)

* **Dioctahedral smectite** /d(06-33)=1.496 Å/ with a basal reflection near 15 Å, i.e. with 2 hydrate layers;
* **Illite, quartz** and **feldspars** in varying amounts along the core;
* **Dolomite** (104):2.89 Å

The quartz and feldspar reflections were as sharp as in the REF sample. Sulphates and iron oxides or hydroxides were not found.

Detailed study of the clay fraction

XRD of oriented material from the clay fraction gave the following conclusions:

REF sample

A characteristic basal reflection d(001)=12.4-12.8 appeared in air-dry condition (Fig.4-6). After Ca saturation and EG treatment peaks appeared at 17 Å (001) and 8.52 Å (002), indicating that MX-80 ED is a pure smectite with no high-charge layers or illite. After K-saturation, and EG treatment complete re-expansion to 16.6 Å (001) and 8.3 Å (002) took place.

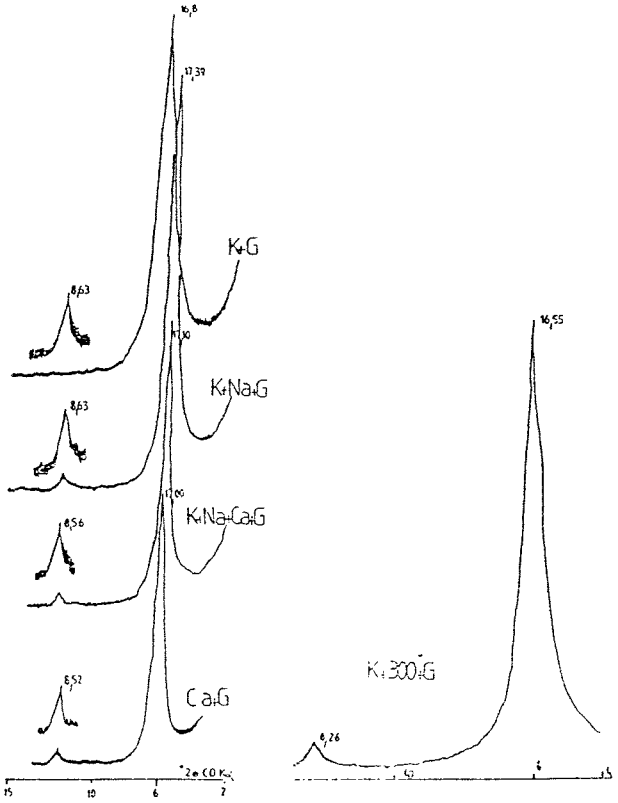

Figure 4-6 Diffractogram of the clay fraction of the REF sample (oriented, air-dry)

IR sample

All specimens showed a single and narrow (001) reflection in the interval 14.66-15.5 Å (cf. Fig.4-7). After Ca-saturation and EG treatment harmonic reflections were found at 16.8-17.3 Å (001), 8.41- 8.53 Å (002), 5.63-5.64 Å (003), and at 3.39 Å (005). These data show that the smectite remained intact with no illitization. After K-saturation and EG treatment a strong (001) peak was found; the (002) reflection appeared at 8.65-8.70 Å and a 10 Å peak also showed up. It was concluded that more than 95 % of the smectite remained intact but that a small amount was converted to high-charge material. This tendency was irregular along the sample, however, indicating some original variation in composition rather than true conversion.

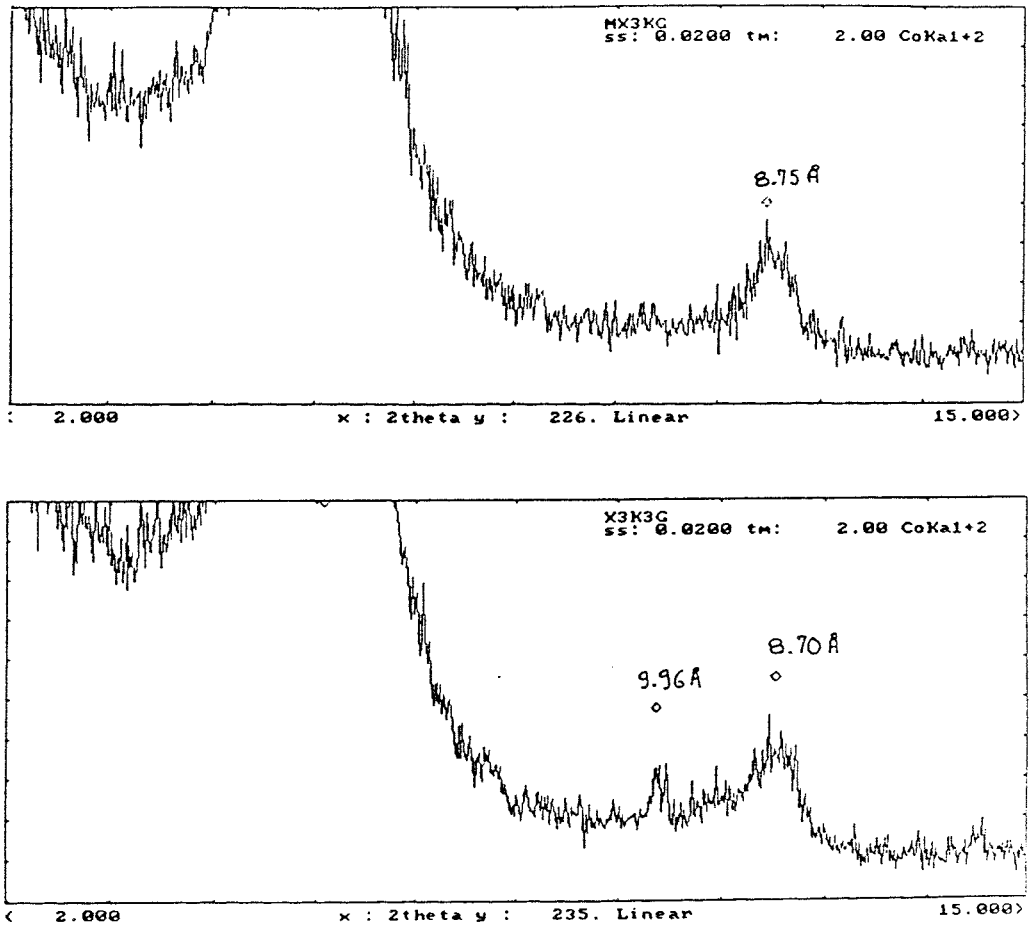

Figure 4-7 Diffractograms of IR sample. Upper: Ca saturation, Lower: K-saturation (oriented, EG-treated)

NONIR sample

The NONIR sample behaved much like the IR sample (Fig.4-8). Thus, under air-dry conditions Ca-saturated specimens showed a single (001) reflection located between 14.5 and 14.9 Å, and after EG treatment this peak was displaced to 16.8-17.3 Å while the (002) reflection appeared in the interval 8.42-8.51 Å. After K-saturation, heating and EG treatment a strong (001) reflection showed up at 17 Å while the (002) reflection was in the interval 8.51-8.58 Å, i.e. slightly higher in the Ca state.

No 10 Å reflections were found, from which it was clear that the low-charge smectite had been practically completely preserved.

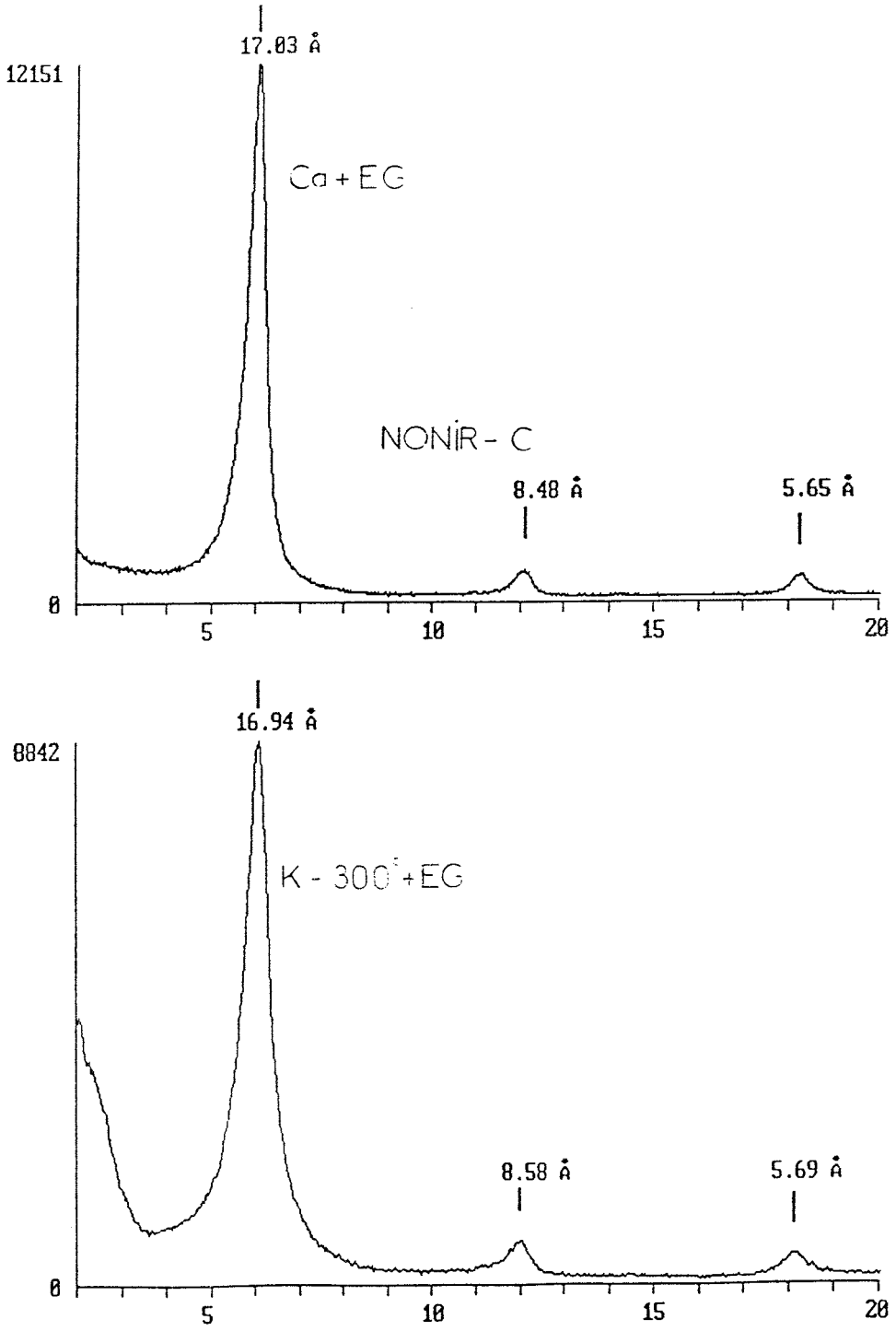

Figure 4-8 Diffractograms of NONIR sample. Upper: Ca saturation and EG treatment. Lower: K saturation, heating to 300°C, and EG treatment

4.2.2 Clay Technology AB study

4.2.2.1 XRD

A condensed picture of the diffractograms of unheated MX-80 and of the 130°C is given in Fig.4-9. It is im-

mediately clear that the most striking effect of the heating and irradiation is the complete disappearance of the feldspar peaks around 2θ = 14°, 24° and 28°. Other obvious differences are 1) a slight increase in 10 Å minerals, 2) broadening towards low angles of the (001) montmorillonite peak in the the 130° specimen, indicating formation of chlorite-type minerals, and 3) appearance of new peaks in this specimen that most probably were caused by neoformation of anhydrate and possibly also hexahydrate, $MgSO_4(6H_2O)$, chlorite, and quartz. The content of kaolinite remained almost constant.

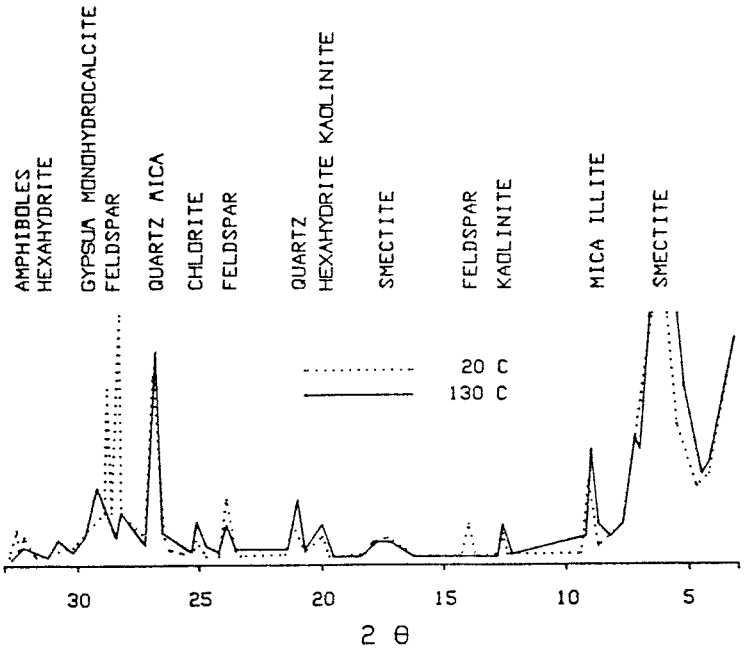

Figure 4-9 Rectified diffractograms of Specimens 00 (20°) and 01 (130°C)

Examination of the diffractograms of specimen 22 (115°C); and specimen 26 (95°) showed that part of the feldspars sustained 95° but that they had almost disappeared at 115°C (Fig.4-10). The amount of 10 Å minerals had increased very little in these specimens while there was a more obvious increase in quartz in the 95°C as manifested by the enlarged peak at 2θ = 21° and 26.7°. The 115°C specimen contained some neoformed gypsum (and anhydrate), of which there was also some sign in the 95°C specimen. The latter may possibly have experienced some neoformation of hexahydrate.

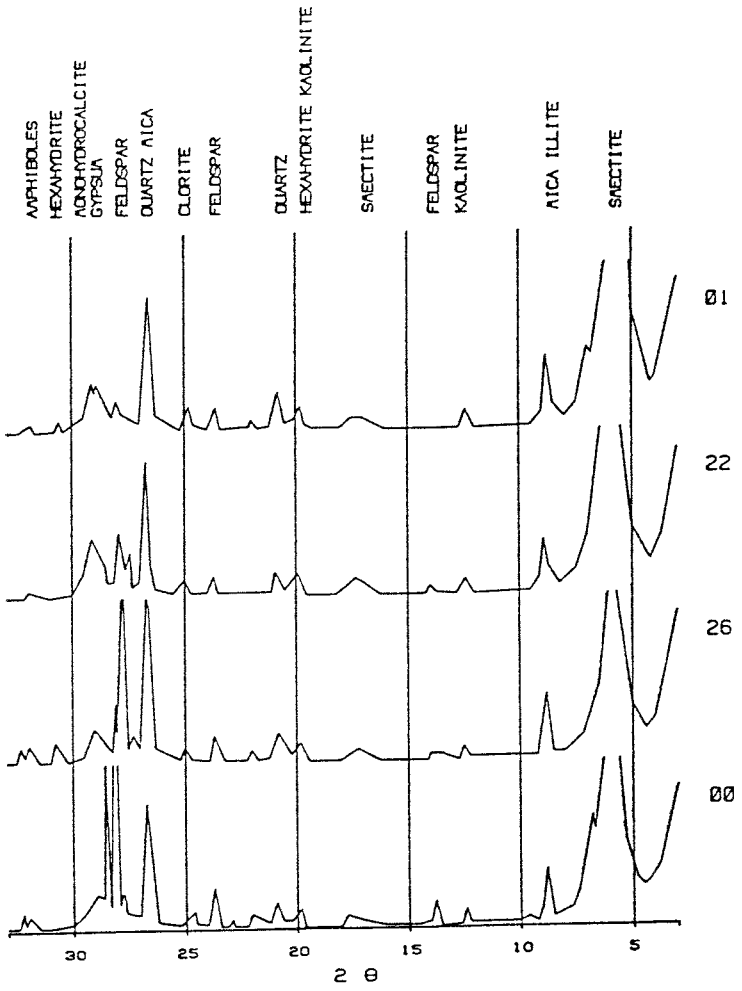

Figure 4-10 Diffractograms of all the specimens

The tendency of broadening of the major smectite peak at $2\theta = 5^{\circ}-7^{\circ}$ towards the low angle region for all the heated specimens, especially the 130 and 115°C ones, was interpreted as resulting from the formation of chloritic minerals. It is probably not a matter of true neoformed chlorite but rather of interlamellar establishment of positively charged, non-stoechiometric iron hydroxide in the smectite stacks, transforming them to chloritic pseudo-forms.

The major interpreted changes of the mineralogy of virgin MX-80 Na montmorillonite are summarized in Table 4-2. The variation in initial mineral composition of the clay makes the interpretation uncertain; except for the slight tendency of formation of 10 Å minerals and for the clear reduction in feldspar as well as the neoformation of sulphates at 130°C.

Table 4-2. Major interpreted changes of the mineralogy of the clay fraction

Specimen no	Reduction	Increase	Change
01 (130°C)	Feldspars		Strong
		Chlorite	Medium
		10 Å min.	Weak
		Anhydrite (+ gypsum)	Strong
		Hexahydrate	Medium
22 (115°C)	Feldspars		Strong
		Chlorite	Weak
		10 Å min.	Weak
		Anhydrite (+ gypsum)	Strong
		Quartz	Weak
26 (95°)	Feldspars		Medium
		Anhydrite	Weak
		Quartz	Weak

4.3 CHEMISTRY

4.3.1 CEA study

4.3.1.1 Composition of bulk samples and clay fractions

The analyses showed that the chemical composition of the bulk and clay fractions were similar (Tables 4-3 and 4-4), which is natural because of the high percentage of smectite in the bulk material.

Table 4-3 Chemical composition of bulk samples

Echantillons	SiO_2	Al_2O3	Fe_2O_3	MnO	MgO	CaO	Na_2O	K2O	TiO_2
REF	58.4	17.6	3.22	0.02	2.12	1.67	3.04	0.53	0.2
IR 1	51.20	17.80	4.90	0.04	3.20	-	2.20	0.77	0.30
IR 2-1	54.60	18.00	4.40	0.03	3.00	-	2.20	0.65	0.30
IR 2-2	54.50	16.70	4.00	0.03	3.00		2.20	0.70	0.35
IR 2-3	54.80	17.50	4.50	0.04	2.30	-	2.20	0.60	0.40
IR 2-4	54.00	17.20	4.20	0.04	2.60	-	2.30	0.70	0.25
IR 2-5	55.00	18.50	4.30	0.04	2.70	-	2.30	0.70	0.35
IR 2-6	54.50	18.70	4.60	0.04	2.80	-	2.40	0.80	0.35
IR 3	55.50	18.00	4.70	0.03	2.70	-	2.40	0.70 .	0.25
NONIR-a	57.00	18.30	4.30	0.01	2.43	0.88	1.95	0.75	0.27
NONIR-b	55.00	18.97	4.13	0.02	2.87	1.09	1.95	0.73	0.33
NONIR-c	56.00	19.40	4.20	0.03	2.96	1.16	1.97	0.76	0.33
NONIR-d	56.00	19.43	4.03	0.02	2.88	1.16	2.00	0.77	0.36
130° contact a	53.90	17.70	6.40	0.02	2.46	0.87	1.82	0.74	0.39

Table 4-4 Chemical composition of clay fractions

Echantillons	SiO_2	Al_2O_3	Fe_2O_3	MnO	MgO	CaO	Na_2O	K_2O	TiO_2
REF	58.4	18.8	3.2	0.01	2.33	1.52	3.33	0.18	0.15
IR-1	53.00	18.40	4.00	0.01	3.10	-	0.60	0.23	0.24
IR-2-1	52.40	18.00	3.60	0.01	3.50	-	1.00	0.30	0.24
IR-2-2	52.90	18.40	3.70	0.02	3.00	-	0.70	0.27	0.25
IR-2-3	53.60	17.80	3.30	0.01	3.00	-	0.50	0.22	0.27
IR-2-4	53.80	18.30	3.60	0.01	2.90	-	0.60	0.22	0.27
IR-2-5	54.00	18.40	3.50	0.02	2.70	-	0.65	0.24	0.26
IR-2-6	52.50	18.70	3.40	0.01	3.00	-	0.40	0.30	0.30
IR-3	51.50	18.50	4.00	0.01	2.80	-	0.80	0.25	0.25
NONIR-a	51.40	17.00	4.40	0.02	2.50	1.40	1.30	0.40	0.25
NONIR-b	50.16	16.90	4.10	0.02	2.50	1.30	1.25	0.40	0.25
NONIR-c	50.50	18.40	4.20	0.02	2.70	1.70	1.20	0.45	0.30
NONIR-d	51.00	17.30	4.20	0.02	2.45	1.10	1.38	0.44	0.26

In comparing the REF material with the IR and NONIR ones one finds that the REF clay had a significantly higher content of Na_2O, CaO, and SiO_2, which can be interpreted as caused by dissolution of feldspars in the heated and irradiated samples. The amounts of Fe_2O_3 had increased throughout the IR and NONIR cores and it was particularly obvious in the NONIR material contacting the steel.

The data in Tables 4-3 and 4-4 include water and if correction is made for this one finds less obvious differences except for the sodium and iron contents (Table 4-5). Taking the initial spread in composition into consideration it is concluded that the changes are insignificant.

Table 4-5 Average chemical composition of REF, IR and NONIR samples with correction for the water content

Samples	SiO_2	Al_2O_3	Fe_2O_3	MgO	CaO	Na_2O	K_2O
REF	68.2	22.0	3.8	2.7	1.8	2.7	0.2
IR	68.4	23.2	4.6	3.7	-	0.8	0.3
NONIR	65.9	21.8	5.6	3.2	1.4	1.7	0.5

4.3.1.2 CEC

The CEC data are given in Table 4-6, from which the following conclusions were drawn respecting mineral conversions:

* The cation exchange capacity was in the range of 80 to 100 meq/100 g of all samples except for the NONIR specimen that had contacted the steel and for one almost centrally located NONIR specimen. Most specimens had higher CEC:s than the reference sample

* IR samples showed a significant drop in exchangeable sodium and magnesium caused by uptake of calcium

* NONIR samples did not show any significant change at all; the most obvious processes were moderate drops in sodium and potassium. The latter may be related to the formation of a very small amount of high-charge smectite

The main conclusion was that the dominant process in the IR core was an exchange of the type:

$$REF\text{-}Na^{+} \text{ ---------->} IR\text{-}Ca^{2+}$$

The drop in exchangeable sodium of the NONIR material is not readily explained; iron emanating from the steel may have replaced at least some of the sodium. Protons may also have played a role.

Table 4-6 CEC analyses (meq/100 g)

Samples	Na	K	Mg	Ca	C.E.C.
REF	56.0	2.3	15.6	30.1	79.3
IR1	20.6	2.4	13.5	50.5	97
IR2-1	26.8	4.2	9.8	49.8	96
IR2-2	24.5	1.7	8.5	53.5	101
IR2-3	12.2	0	8.5	63.2	95.4
IR2-4	24.0	1.4	8.6	54.2	94.3
IR2-5	18.0	1.4	7.3	43.5	100
IR2-6	7.5	1.6	9.8	53.4	104
IR3	34.6	1.7	10.4	36.4	92.5
NONIR a	41.25	2.00	11.52	24.7	94.43
NONIR b	30.43	1.4.5	11.14	17.0	59.29
NONIR c	30.48	1.47	12.88	28.9	84.05
NONIR d	43.22	1.78	11.03	24.8	75.83

4.3.1.3 FTIR

All the recorded spectra are almost identical as illustrated by Figs.4-11 and 4-12. In the high-frequency zone a major band is observed near 3630 cm^{-1} with a shoulder at 3690-3700 cm^{-1}. These bands, which are characteristic of smectite, are attributed to valence vibrations of Al2-(OH) and Al-Mg(OH) groups. In the low frequency zone lattice vibrations including Si-O and Si-O-M bands are observed at 1120, 1040, 622, 525 and 466 cm^{-1}. No significant modifications of frequencies were found among the spectra.

Banding modes of (OH) vibrations are recognized more clearly in the low-frequency zones and one can identify the following ones: Al2(OH): 917 cm^{-1}, Al-OH-Fe: 887 cm^{-1}, and Al-OH-Mg: 850 cm^{-1}, the shape and intensity of which are about the same in all the spectra. The two bands located at 798 and 779 cm^{-1} are attributed to Si-O vibrations in SiO_2 compounds (quartz, opal), the intensities varying as a function of the amounts of such compounds in the samples.

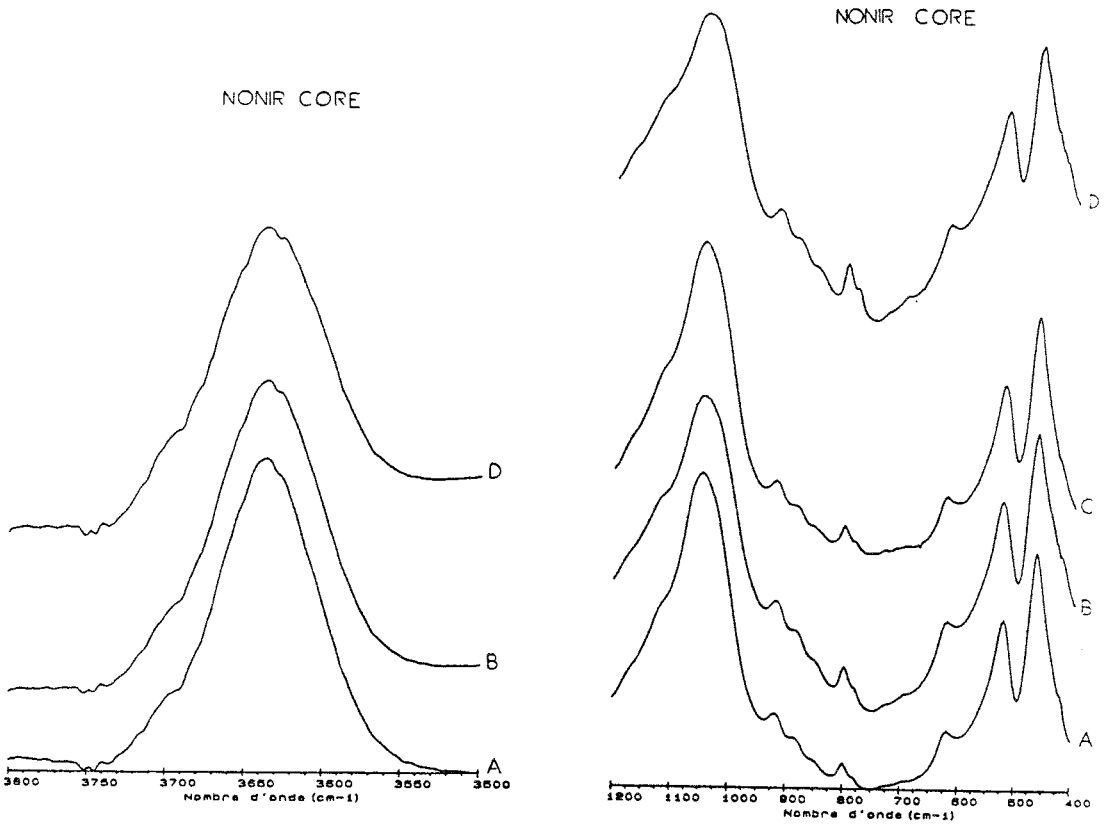

Figure 4-11 FTIR spectra of NONIR materials

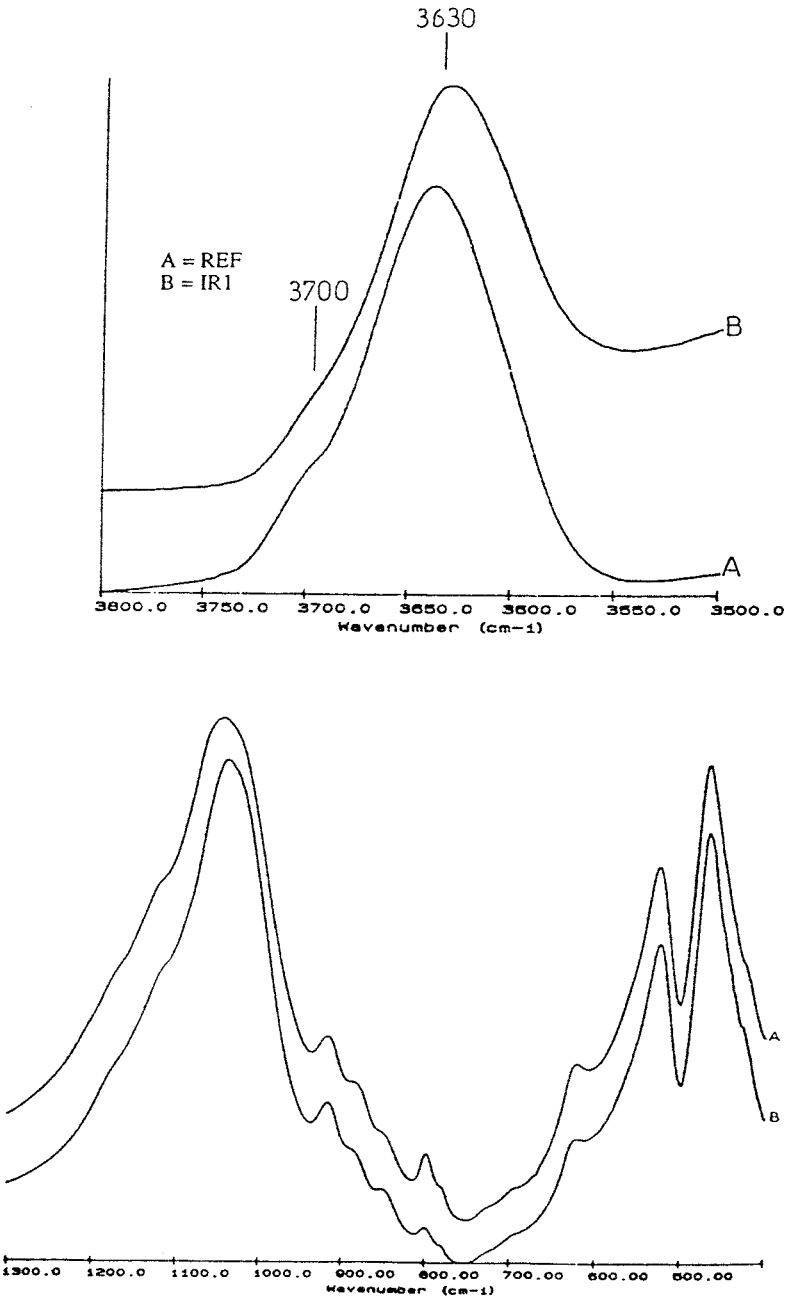

Figure 4-12 FTIR spectra of REF and IR materials

4.3.1.4 Mössbauer data

REF

The REF sample gave a spectrum showing one asymmetric doublet centered at about +3 mm/s, a correct fit being obtained only with a doublet containing two Lorentzian lines of equal width (Fig.4-13). The Mössbauer parameters of this fit show that the smectite contains only Fe^{3+} in octahedral positions (Table 4-7), meaning that the REF material did not contain any Fe^{2+} cations. No signal indicating the presence of crystallized iron oxides or hydroxides could be observed.

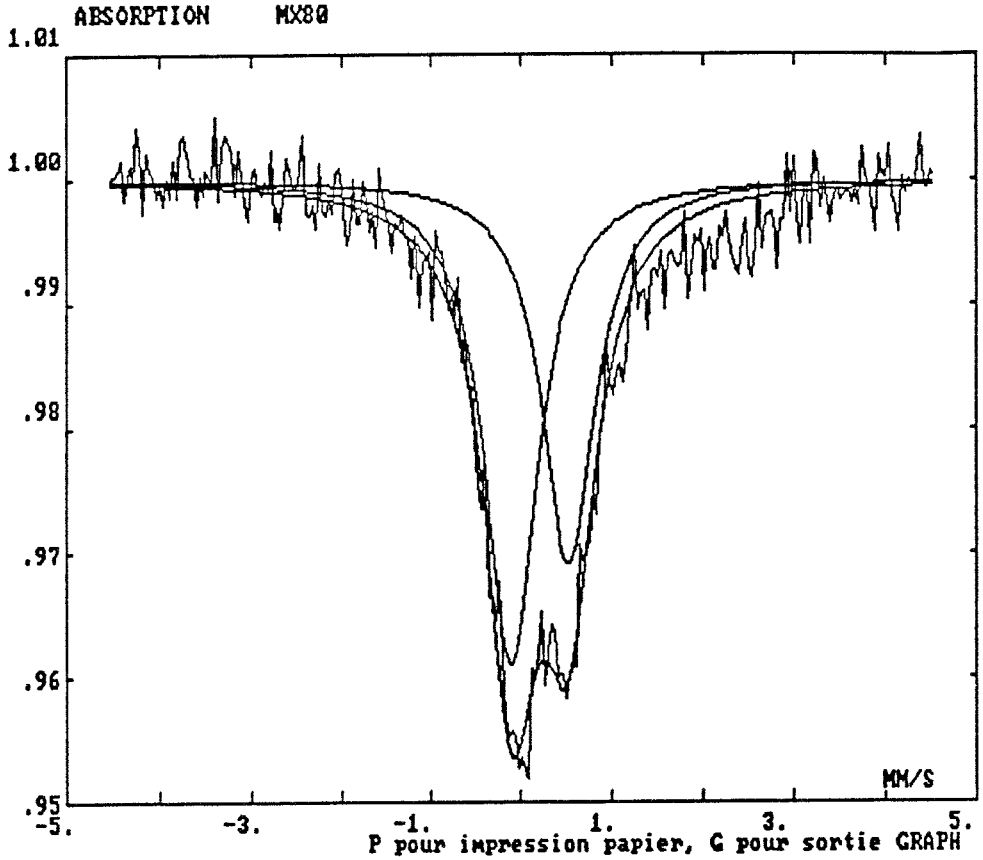

Figure 4-13 Mössbauer spectrum of the REF material

Table 4-7 Mössbauer parameters

Sample	Fe3+ octahedral				Fe2+ octahedral			
	δ	Δ	Γ	S	δ	Δ	Γ	S
REF	0.325	0.622	0.79	100				
MX80.ED	0.30	0.67	0.7	83	1.15	2.83	0.6	17
IR1	0.36	0.663	0.75	81	1.14	2.78	0.47	19
IR2-1	0.31	0.686	0.66	72	1.28	2.68	0.73	28
IR3	0.36	0.608	0.56	85	1.1	2.84	0.48	15
NONIR A	0.32	0.654	0.65	85	1.34	2.43	0.5	15
NONIR B	0.31	0.67	0.70	78	1.20	2.55	0.6	22

δ = isomer shift
Δ = quadrupole splitting
Γ = full line width
S = relative area

Since the mineralogical variations in the MX-80 ED material appeared to be rather significant, other samples of this clay material than the REF material were analyzed as well and all of them appeared to yield somewhat different Mössbauer spectra as indicated by Fig.4-14. The spectra can be fitted with two doublets, one corresponding to Fe^{3+} cations in octahedral positions and the other to Fe^{2+} in such positions. About 15-20 % of the iron is in ferrous form. Since the clay fraction of MX-80 ED did not contain carbonates or micaceous phases, all iron was assumed to be located in the smectite clay lattice.

IR

The spectra of the IR material, specimens 1, 21 and 3 (located as shown in Fig.4-1), appeared to be practically identical and could be fitted with two doublets (Fig.4-15). This gave the conclusion that the iron in the IR material contained from 15 to 28 % Fe^{2+} cations. No well crystallized iron oxy-hydroxides could be identified.

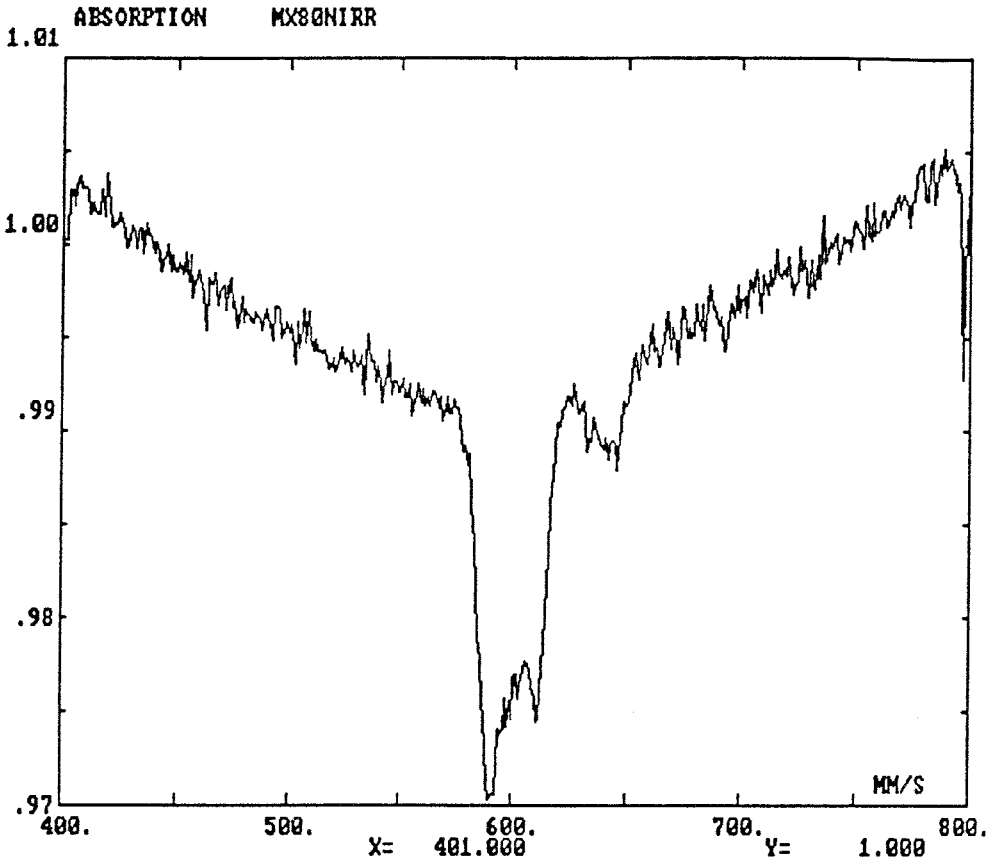

Figure 4-14 Example of variation in Mössbauer spectra of MX-80 ED material

NONIR

All the specimens from the NONIR sample gave the same Mössbauer spectra, which fitted well with two doublets (Fig.4-16). As for the IR material Fe^{2+} cations represent about 15-25 % of the iron. Well crystallized iron oxide or hydroxide was not present.

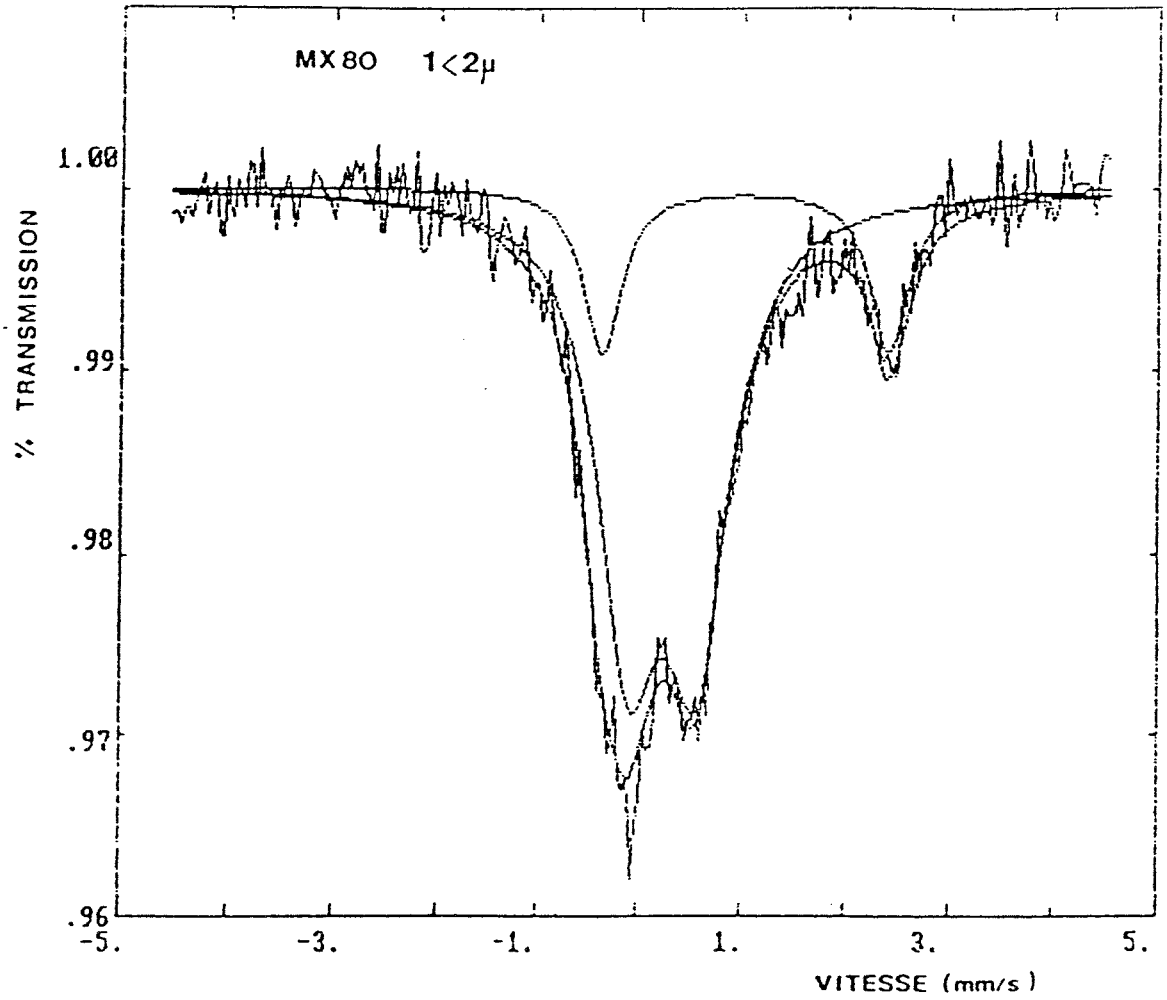

Figure 4-15 Mössbauer spectra of IR material

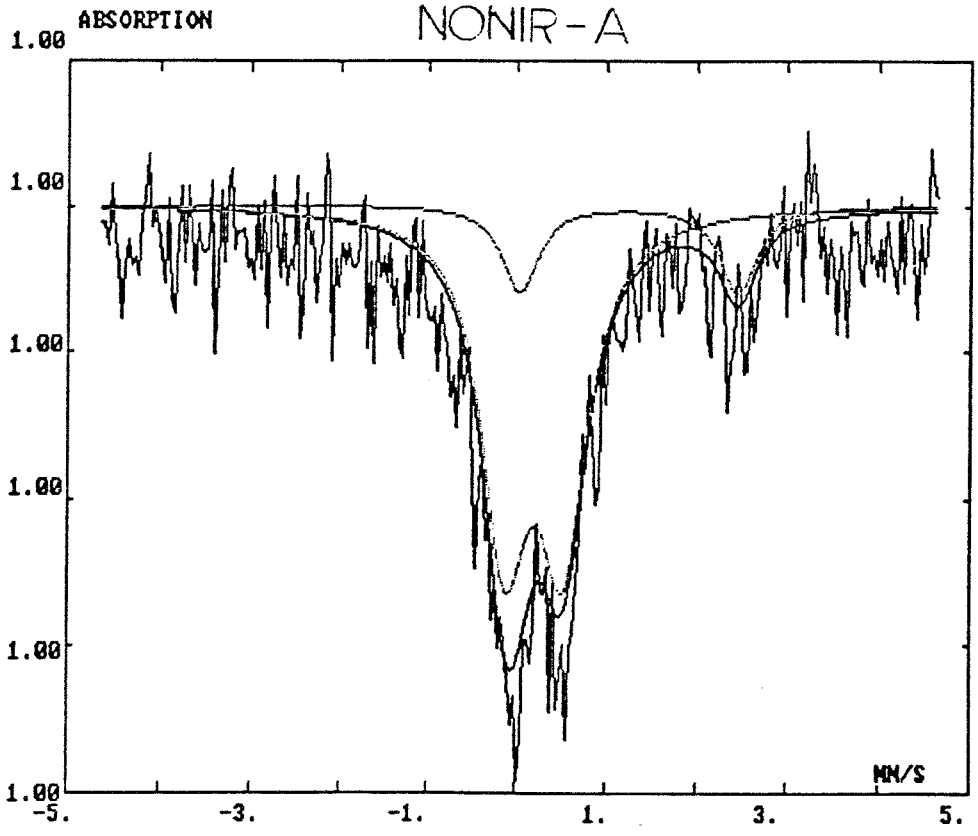

Figure 4-16 Mossbauer spectra of NONIR material

4.3.1.5 ESR data

The investigated material was the clay fraction of the REF sample and all the specimens from the IR and NONIR samples. A general conclusion is that the recorded signals are typical of montmorillonite as illustrated by Fig.4-17.

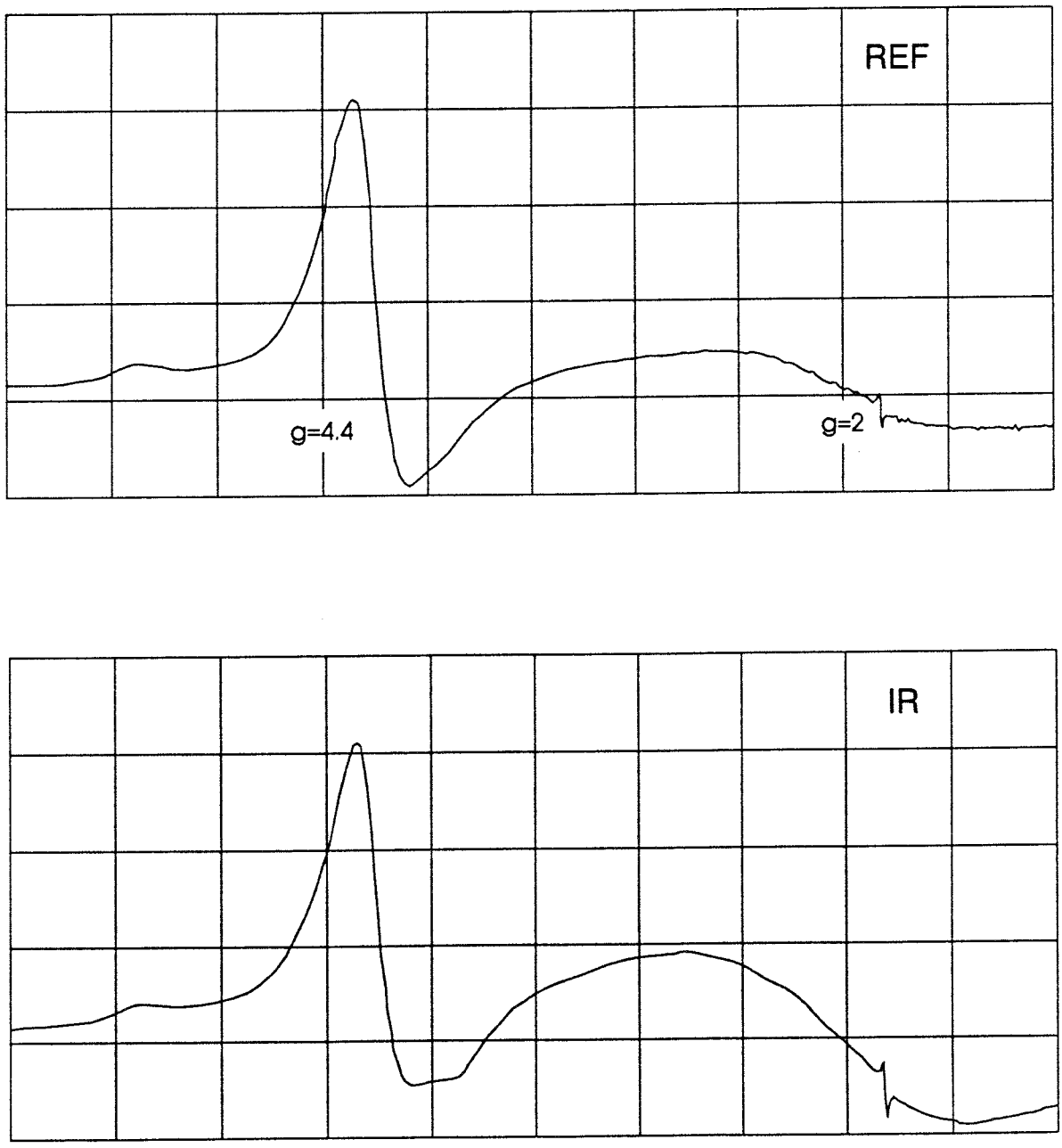

Figure 4-17 ESR spectra. REF and IR materials (clay fractions)

The following features could be identified:

* The narrow line at g=4.4 indicates Fe^{3+} atoms in octahedral sites, dispersed in sheets that contains aluminum and magnesium

* The broad band centered at g=2 refers to near-neighboring Fe^{3+} atoms. This indicates that the small amount of iron in MX-80 ED is present as oxides or hydroxides

* The very narrow line at g=2 is interpreted as defect centers in the smectite lattice since significant amounts of organic material - which would otherwise show such a feature - were not present

The ratio of the intensity of the signal caused by defect centers and that at g=4.4 is about 0.08 for both the REF and the NONIR materials, while it is 0.20 for the IR material, which shows that irradiation had produced an increase in the number of defect centers.

4.3.2 Clay Technology AB study

4.3.2.1 Composition of bulk samples

As in the mineralogical study performed by Clay Technology, the intention was to identify whether major changes had taken place that could explain differences in the physical properties of reference material and the material exposed to heat combined with irradiation, and not to get information on detailed changes.

The spectrometric analyses of $LiBO_2$ melts shown in Table 4-8 indicate that the major elements are present in approximately unaltered proportions in all the specimens, except for iron, which is enriched in the 130°C and the 115°C specimens. There may be a slight net loss in SiO_2 in all the specimens, especially in the hottest one, and some silica may have migrated out of the system due to the concentration gradient. However, the precipitations noticed in the TEM study and the assumed neoformation of quartz suggests that silica was released from dissolving montmorillonite and accessory silicate minerals had precipitated in the sample. It should be noted that this study, like CEA's, did not show the reduction in sodium at the hot end that appeared in the non-irradiated sample.

Table 4-8. Major element composition of clay specimens (solid mass and contained in water), in %. The values are corrected for the ignition loss

Specimen	SiO_2	Al_2O_3	Fe_2O_3	MgO	K_2O	CaO	Na_2O
00 (Ref)	64.4	21.0	4.7	3.0	0.9	2.0	2.5
01 (130°C)	63.5	21.2	5.9	3.3	0.8	1.8	2.4
22 (115°C)	64.1	21.4	5.5	3.2	0.8	2.1	2.4
26 (95°C)	63.7	22.4	4.9	2.9	0.8	2.3	2.6

One finds that a significant increase in iron content took place in the 130°C specimen and some increase was also noticed for the one exposed to 115°C. Part of this iron is assumed to have formed cementing precipitates, while some is assumed to have been used up in the formation of chloritic minerals. Theoretically at least, montmorillonite may have partly transformed to nontronite.

Although it is not very significant there seems to be an uptake of magnesium in the hottest parts of the clay sample. This enrichment may have been caused by Mg being taken up in octahedral positions in conjunction with some transformation of montmorillonite to high-charge smectite at the hottest end. This would have enhanced the release of silica from this end and caused some I/S mixed-layer formation, where I may simply have been montmorillonite stacks collapsed to 10 Å minerals and prevented from expanding by cementing silica precipitates. Another possible cause of the Mg enrichment may be formation of magnesium sulphate.

Pyrite, being a natural constituent of the bentonite, was dissolved, by which sulphur was set free to interact with calcium and magnesium to form sulphates like anhydrite in the hotter parts of the sample.

4.3.2.2 CEC

Determination of the Sr uptake on strontium solution treatment gave the CEC-values in Table 4-9.

Table 4-9. CEC -values

Specimen	CEC, meq/100 g
00 (Ref)	99
01 (130°C)	93
22 (115°C)	92
26 (95°C)	97

One concludes from the CEC-measurements that the changes are small and that valuable information on actual mineralogical changes is hardly offered by this sort of analysis except that the amount of smectite cannot have been significantly reduced.

4.3.2.3 Microstructural properties

A general conclusion from the TEM study is that all the specimens showed the characteristic microstructural features of dense smectite clay formed from granulated powder, i.e. stacks of flakes ("aggregates") separated by voids in which softer clay gels are hosted. The latter may either be flakes or stacks released from the dense aggregates, or neoformed crystalline or amorphous aluminosilicates.

However, while the general appearance of heated and unheated virgin material turned out to be very similar, a careful examination showed a number of different features (Fig.4-18). The major one is that the unheated reference material exhibited a rather low degree of homogeneity while all the other showed a more homogeneous structure, which is in good agreement with earlier experience (Fig.7). Still, it seems that the most strongly heated specimen 01 had a somewhat higher frequency of dense aggregates, possibly representing stacks of montmorillonite flakes that had collapsed to 10 Å units.

Further obvious differences are that specimen 01 heated to 130°C and specimen 22 heated to 115°C showed a number of precipitations, the first-mentioned clay sample being particularly rich in such objects (Fig.4-19). The morphology and EDX analysis suggest that anhydrite (or gypsum), and calcite (probably monohydrocalcite as indicated by the XRD analysis) were the major neoformed species.

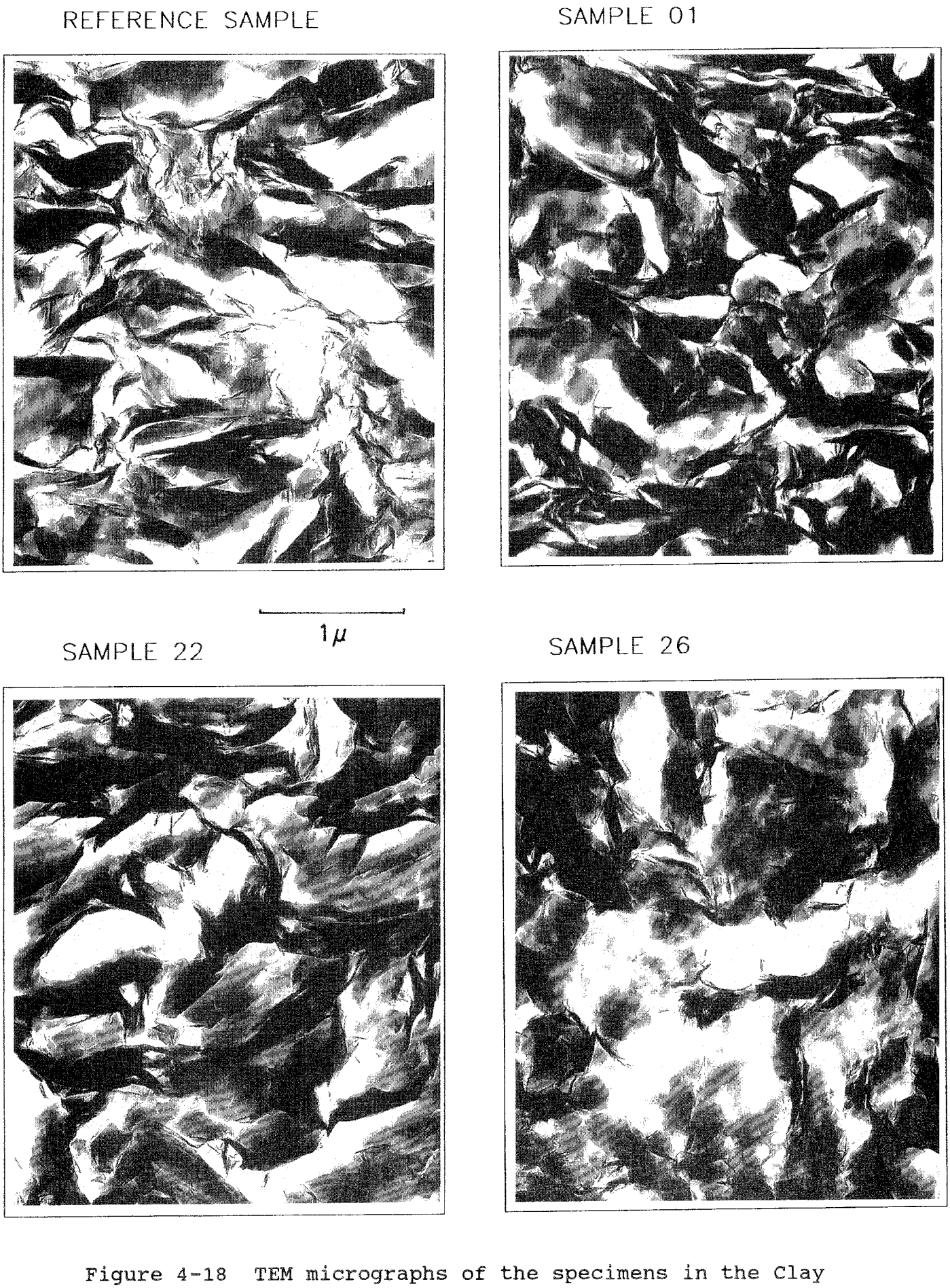

Figure 4-18 TEM micrographs of the specimens in the Clay Technology study

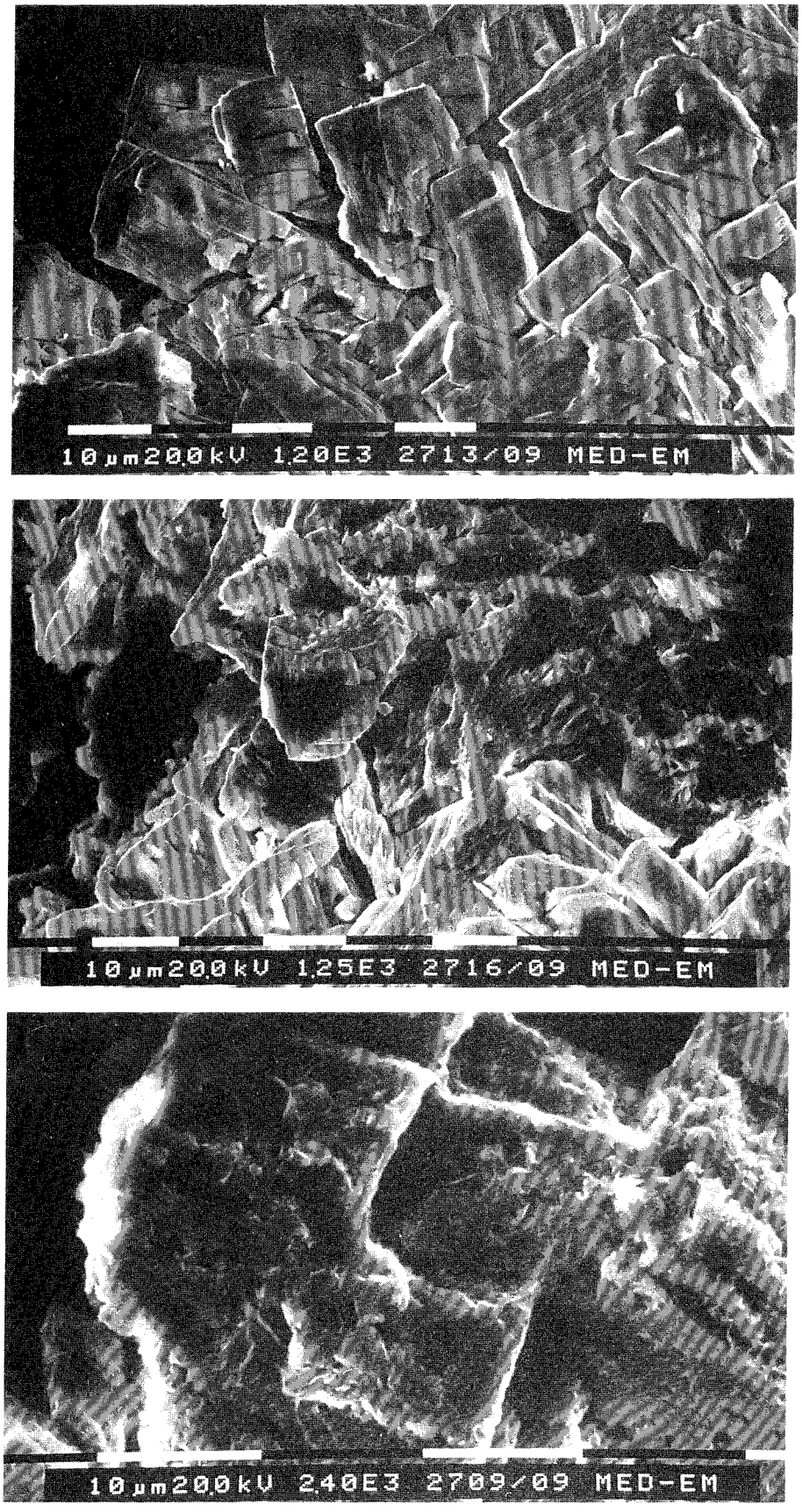

Figure 4-19 Precipitations in the 01 specimen, heated to 130°C. Upper and center: Calcium sulphate. Lower: Precipitates rich in iron and calcium

4.3.3 Conclusions and discussion of mineralogical and chemical changes caused by heating and irradiation

4.3.3.1 Initial composition of MX-80 ED

A major conclusion that makes it difficult to draw definite conclusions concerning the mineral changes that took place in the heat and heat/irradiation experiments is that the MX-80 ED material is not very homogeneous. Thus, while the smectite content is very high, i.e. more than 80 %, it varies somewhat as does the content and composition of accessory minerals. These consist of quartz and feldspars, illite, opal, gypsum, calcite, dolomite and hematite.

An important fact is that the iron content is low and that most iron is present as octahedral Fe^{3+} while about 20 % seems to form octahedral Fe^{2+}.

4.3.3.2 Heat- and irradiation-induced changes

The CEA study showed the following major effects:

* - **Irradiation combined with heating** caused disappearance of calcite and considerable loss in quartz and feldspars. Ferric iron phases appeared at the two steel contacts, where poorly crystallized hematite was formed. The diffusion rate of iron in the sample was rather significant.

  - A significant drop in Na_2O content took place particularly at the hot end.

  - The smectite content was very little affected; there was no clear indication neither of dissolution or crystal growth. However, a small amount of high-charge smectite seems to have formed as a separate phase.

  - The changes that could be observed appeared to be quicker than in the non-irradiated, heated experiment.

  - The irradiation caused more crystal lattice defects than only heating.

* - **Heating without irradiation** caused nearly the same changes as when irradiation was also applied, but they were slower and less well developed.

  - Crystal lattice defects were not caused.

The Clay Technology AB study, which only concerned the sample with combined irradiation/heating, showed the following major effects:

* Strong drop in feldspar content at the hot end and also a clear reduction in the rest of the clay core.

* Significant formation of sulphates at the hot end, primarily hexahydrate and anhydrite with Ca stemming from dissolved feldspars and probably calcite, and sulphur from dissolved sulphide minerals.

* Slight increase in quartz throughout the sample, the probable reason being recrystallization of silica released from feldspars.

* Tendency of chlorite formation in the hottest half of the clay core, the steel possibly supplying iron for this process.

4.3.3.2 Conclusions

Putting together the information from the studies, it seems clear that the dioctahedral mineral montmorillonite underwent insignificant changes in the one year long experiment with combined heating and irradiation, the effects being even smaller when only heating was applied.

The accessory minerals, however, were very significantly altered, creating free silica that became available for cementing processes. Also, iron stemming primarily from the most strongly heated, irradiated steel, is concluded to have taken part both in cation exchange processes and in the formation of iron compounds serving as cement.

4.4 PHYSICAL PROPERTIES

4.4.1 Hydraulic conductivity

The hydraulic conductivity was found to be of the same order of magnitude as that of reference MX-80 clay (cf. Table 4-10)). The slight difference in conductivity is within the accuracy of measurements.

Table 4-10 Hydraulic conductivity

No	Temp. °C	Dist.fr.iron plate cm	Hydr. cond. m/s
00	Ref.	-	1.7×10^{-13}
01	130	0.5	2.9×10^{-13}
22	115	2.5	1.1×10^{-13}
26	95	5.7	2.6×10^{-13}

The evaluated hydraulic conductivities are very close to those generally found for MX-80 clay prepared and percolated by low-electrolyte water (3). It is concluded that there is no definite trend of a changed conductivity with increased temperature and irradiation.

4.4.2 Rheology

Creep curves of the specimens are shown in Figs.4-20 4-23. They are all very smooth, indicating that cementation was insignificant. Taking $t = 10^5$ s as a reference time, one obtains the accumulated strain ε shown in Table 4-11 for the four specimens, the table also showing the evaluated A, B, and t_o-values. Generally expressed, high B-values indicate large deformability, while low ones indicate strengthening and stiffening by cementation or homogenization, usually accompanied by a very low or negative t_o (2).

One finds that the specimen 01, i.e. the one exposed to 130°C and the strongest radiation, and also being in close contact with the iron plate, had undergone considerable strengthening. Also specimen 22, which was located a couple of centimeters from the iron plate and heated to 115°C, experienced some strengthening. In contrast, specimen 26 which was heated to 95°C, seems to have become slightly more deformable than untreated MX-80 as manifested by the higher B-value. However, its t_o-values are lower than those of the reference sample, which means higher strain rates on load application, probably indicating slight cementation.

Table 4-11 Rhelogical data (Ref. time for ε is 10^5 s)

"EFFECTIVE" SHEAR STRESS 260 kPa

No	Temp. °C	Dist.fr. irr. steel cmx10^4	ε	A	B	t_o s
00	Ref.	-	$5x10^{-4}$	16	2.1	8000
01	130	0.5	$2x10^{-4}$	-2	0.4	240
22	115	2.5	$4x10^{-4}$	-3	0.9	1460
26	95	5.7	$10x10^{-4}$	-17	2.8	2570

"EFFECTIVE" SHEAR STRESS 520 kPa

00	Ref.	-	$16x10^{-4}$	-22	3.7	1610
01	130	0.5	$12x10^{-4}$	-10	2.4	770
22	115	2.5	$23x10^{-4}$	-9	3.5	100
26	95	5.7	$27x10^{-4}$	-22	5.0	440

The similar trend for both stress levels of the parameter B, which is the most important one, indicates that the shear resistance of the most strongly heated and irradiated part of the clay core was definitely increased, but the increase was very moderate and the ductile behavior of the entire clay core was largely preserved. This is confirmed by the fact that t_o was not altered to become negative even of the part that was exposed to the highest temperature and radiation.

4.4.3 Expansion tests

The tests involved measurement of the spontaneous expansion of laterally confined clay samples when the initial effective pressure 6 MPa was reduced to 5 MPa, the samples being exposed to Allard water through a filter stone. The results are plotted in the diagram of Fig.4-24, from which one finds that the expansion took place in a smooth, continuous fashion. This indicates that significant cementation had not taken place in any of the specimens. Also, it is clear that the unheated reference sample and the 130°C specimen 01, which had been most strongly affected by radiation, behaved similarly and that the latter had an expandability that was even somewhat higher than that of specimens 22 and 26. Since cementation can hardly have affected specimens 22 and 26 more than specimen 01, a possible explanation may be that irradiation had caused disintegration and a drop in particle size and, hence, an increase in specific surface area. This matter is further discussed later in the report.

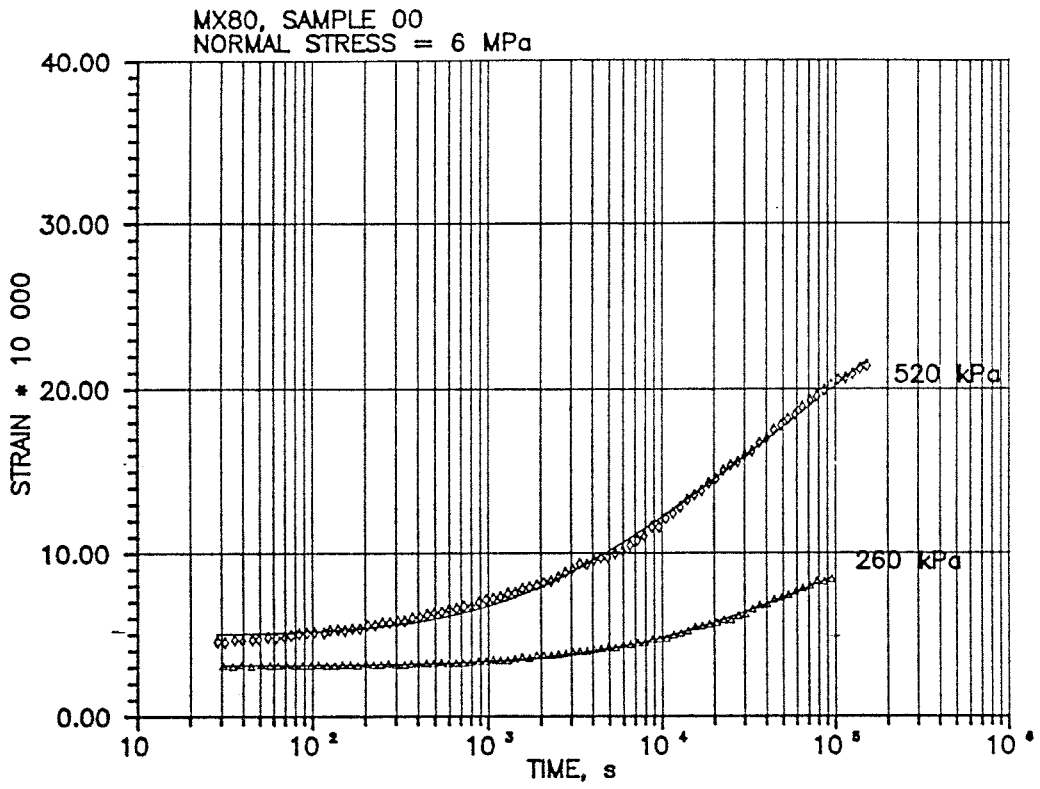

Figure 4-20 Creep curves of Reference Sample

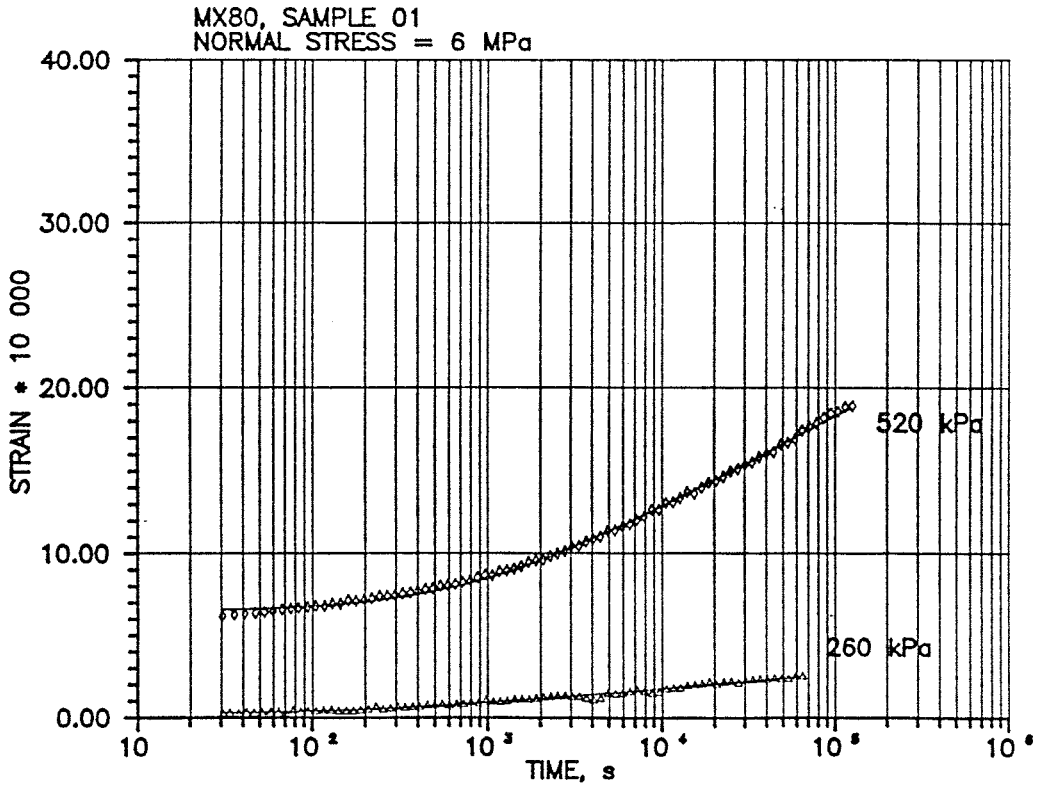

Figure 4-21 Creep curves of specimen 01, heated to 130^{o}C

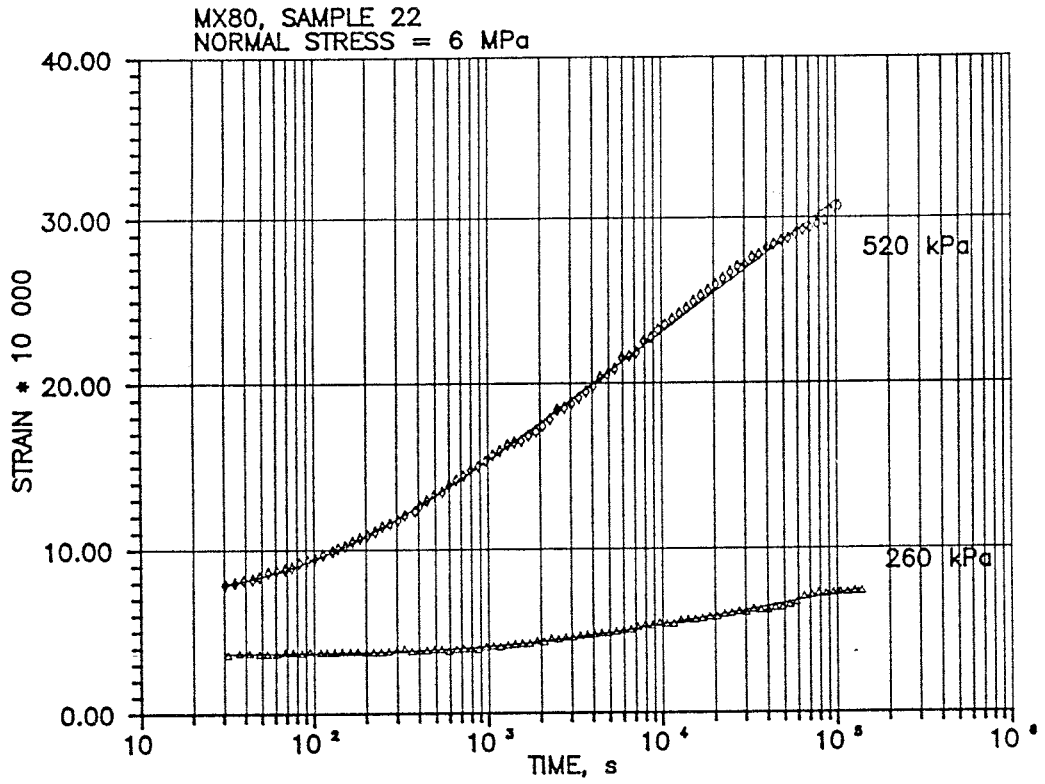

Figure 4-22 Creep curves of specimen 22, heated to 115°C

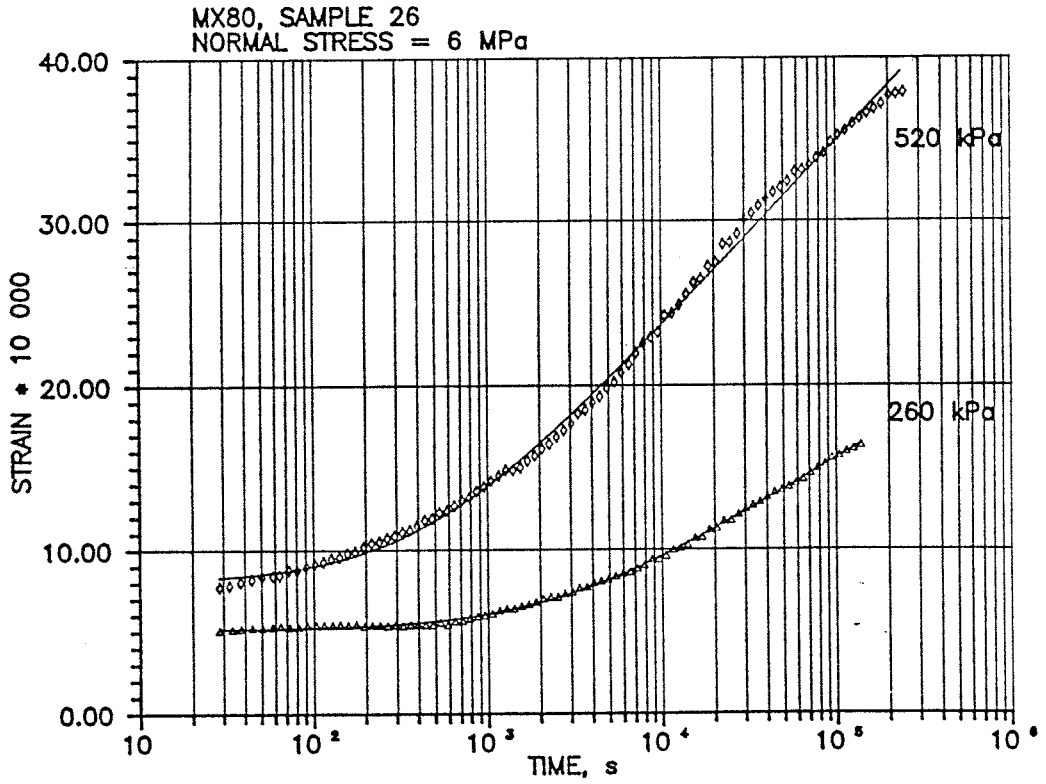

Figure 4-23 Creep curves of specimen 26, heated to 95°C

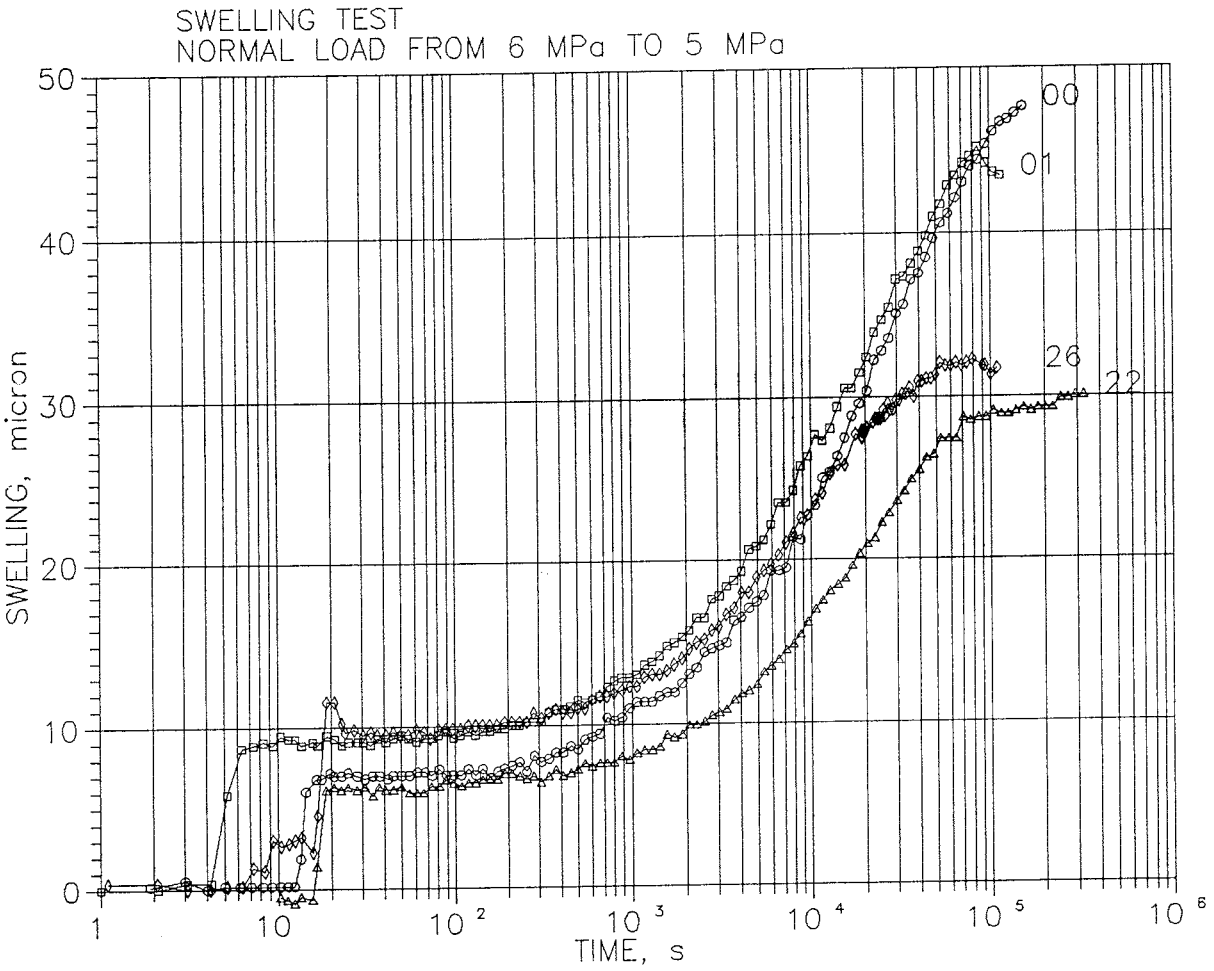

Figure 4-24 Swelling tests under uniaxial conditions

4.4 STEEL CORROSION

The steel at the most strongly heated end of the irradiated and non-irradiated clay cores was investigated by CEA, applying thin section technique. Figs.4-25 and 4-26 illustrate the corroded profile of the heated and irradiated clay, while Fig.4-27 shows the steel which was only subjected to heating (130°C).

It was concluded that the corrosion of the heated and irradiated steel had taken place locally to 480 μm depth. The average depth was 80 μm (Figs.4-25 and 4-26). The steel/clay boundary appeared to be very irregular and a 10-20 μm thick dark zone of enriched, presumably iron-rich matter was identified.

The non-irradiated steel showed somewhat less degradation (Fig.4-27): the maximum corrosion depth was 160 μm and the average depth 18 μm.

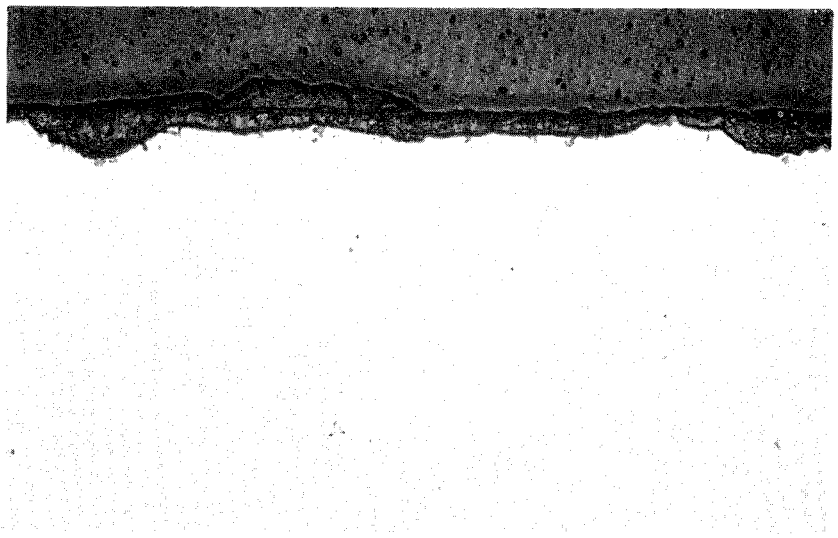

X 65

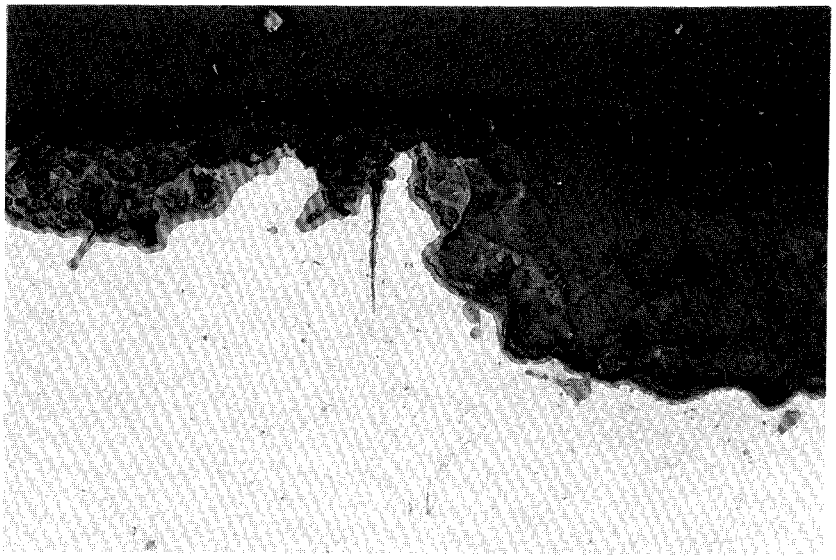

X 125

Figure 4-25 Steel surface that had contacted MX-80 ED clay in the heated (130°C) and irradiated case. Magnifications 65 and 125 x. The steel is shown white

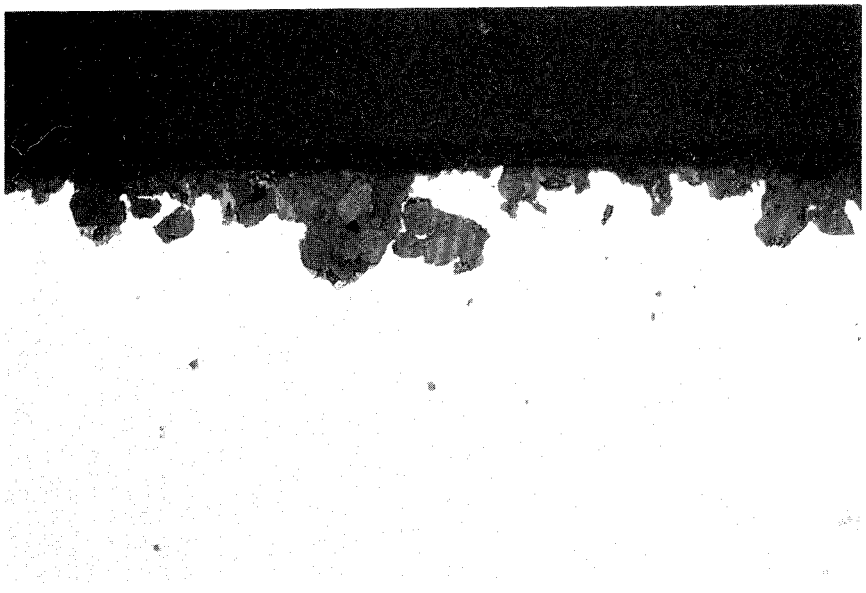

x 250

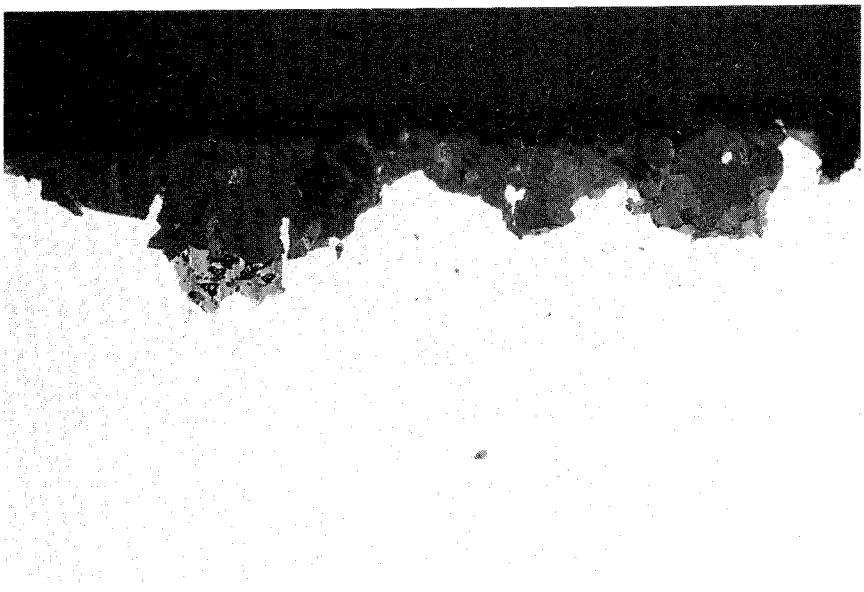

x 250

Figure 4-26 Steel surface that had contacted MX-80 ED clay in the heated (130°) and irradiated case. Magnifications 250 x. The steel is shown white

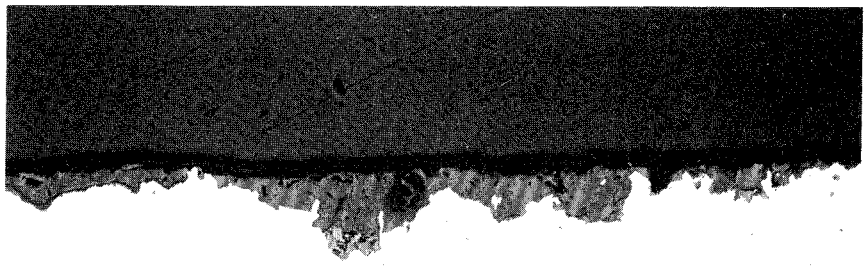

x 125

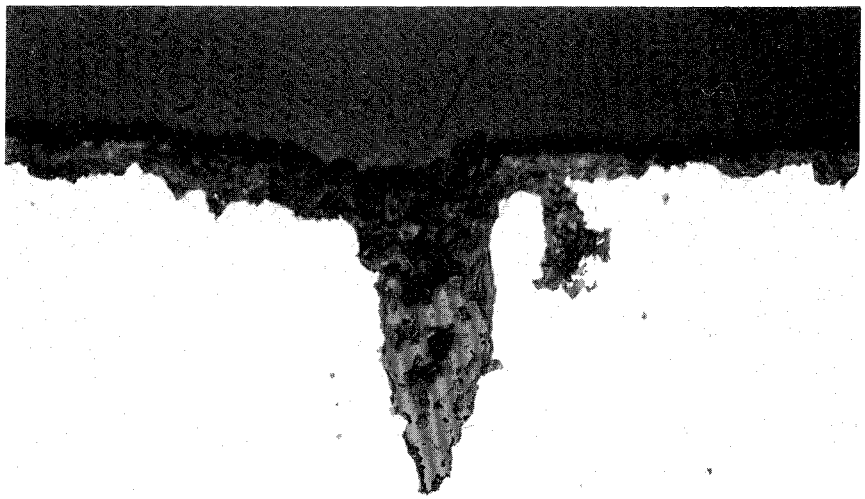

x 125

Figure 4-27 Steel surface that had contacted MX-80 ED clay in the heated (130°) case without irradiation. The steel is shown white

5 DISCUSSION AND CONCLUSIONS

5.1 EFFECTS OF HEAT AND IRRADIATION ON THE MINERALOGY OF THE CLAY

It seems probable that several processes took place that had some but rather small effect on the montmorillonite content in the clay in the hottest part of the clay core. Thus, it seems possible that a small portion of the montmorillonite was converted to high-charge smectite like beidellite (4), yielding some free silica that contributed to the slight cementation that took place at the hot end of the irradiated sample. It may also be a matter of permanent collapse to 10 Å minerals, appearing as paragonite-type minerals, of a small fraction of the montmorillonite content in conjunction with drying at the steel/clay contact despite the high water pressure (5). Hydrogen gas formed at the corrosion of the steel may well have displaced water and caused drying (6).

The silification, i.e. precipitation of silicious compounds that caused the slight cementation in the most strongly heated and irradiated part of the sample may also have originated from the dissolution of feldspars.

Iron released from the corroding steel in the most strongly heated and irradiated part of the clay core seems to have migrated rather far in the clay and may have taken part in several processes. Cation exchange and formation of amorphous oxy-hydroxide iron complexes contributing to the slight cementation are two probable processes and intercalation of iron compounds yielding some transformation of the montmorillonite to chlorite-type minerals is also possible.

Neoformation of calcium- and magnesium-bearing sulphates at the hot end, and the very obvious drop in feldspar content are the two most significant changes among the non-clay minerals. The precipitation of sulphates may actually also have contributed to the cementation process.

5.2 IMPACT OF HEAT AND IRRADIATION ON THE PHYSICAL PROPERTIES OF THE CLAY

A general conclusion is that the one-year long hydrothermal test with rather strong γ radiation did not alter the physical properties very significantly. Thus, the hydraulic conductivity remained unchanged and the rheological behavior only underwent moderate or small changes, meaning that cementation effects were not very important and that the swelling ability did not decrease significantly.

Still, appreciable strengthening of the clay within 1 - 2 cm distance from the steel plate took place and it may lead to brittleness and fracturing at prolonged exposure to heat in the near vicinity of a steel canister in a repository (6).

5.3 IMPACT OF IRRADIATION ON THE CLAY

5.3.1 Gas production

Radiolysis must have been caused in the experiment, meaning that H^+, H_2, OH, H_2O_2 and HO_2 were primary products formed in the porewater, and that O_2^- and O_2 were secondary products. The oxygen produced in the sample is assumed to have supported corrosion of the steel, forming iron hydroxide and hydrogen gas, as well as iron in ionic form. The hydrogen gas of which some may have been released by diffusion, may have filled a large fraction of the clay voids at the steel contact and thereby retarded the corrosion process. No channel-like discontinuties through which gas under high pressure can have left the clay/steel contact were found in the microstructural analysis, visual examination or hydraulic testing.

5.3.2 Influence of radiation on clay minerals

The direct effect of very strong γ radiation is known to be very small but that it tends to cause lattice breakdown and transfer from crystalline state to amorphous conditions of minerals (7). Aluminum has been reported to be replaced by protons, yielding lattice instability. Another finding is that the average particle size decreases because of the lattice instability and this creates an increased specific surface area. If this took place in the presently described experiments it may have produced a high hydration power and swelling ability in the most heated and irradiated clay despite the cementation and slight drop in montmorillonite content.

5.4 IMPACT OF HEAT AND IRRADIATION ON STEEL CONTACTING CLAY

A major conclusion was that irradiation speeds up the corrosive attack on steel caused by heating, and that the corrosion depth becomes larger than with heating only. The corrosion and the release of iron from the corroded steel is on the same order of magnitude as in field and laboratory experiments described in literature (6,8,9).

6 REFERENCES

1 **Pusch,R.**
A Technique for Investigation of Clay Microstructure.
J. de Microscopie, Vol.6, 1967

2 **Pusch,R., Börgesson, L. & Erlström,M.**
Alteration of Isolating Properties of Dense Smectite Clay in Repository Environment as Examplified by Seven Pre-Quaternary Clays.
SKB Technical Report 87-29, SKB, Stockholm, 1987

3 **Pusch,R., Karnland,O. & Hökmark,H.**
GMM - A General Microstructural Model for Qualitative and Quantitative Studies of Smectite Clay.
SKB Technical Report 90-43, SKB, Stockholm, 1990

4 **Pusch,R., Karnland,O., Hökmark,H.,Sanden,T. & Börgesson,L.**
Final Report of the Rock Sealing Project - Sealing Properties and Longevity of Smectitic Clay Grouts.
Stripa Project Technical Report 91-30, SKB, Stockholm, 1991

5 **Pusch,R. & Karnland,O.**
Preliminary Report on Longevity of Montmorillonite Clay under Repository Conditions.
SKB Technical Report 90-44, SKB, Stockholm, 1990

6 **Pusch,R. et al.**
Final Report on SKB/CEAHydrothermal Field Test with French Candidate Clay Embedding Steel Heater in the Stripa Mine.
SKB Technical Report, 1992 (In preparation)

7 **Ewing,R.C., Haaker,R.F., Headly,T.J. and Hlava,P.F.**
Scientific Basis for Nuclear Waste Management, ed. Topp,S.V. Elsevier, N.Y. 1982

8 **Miwa,K., Kanno,T., Asano,H. & Wakamatsu,H.**
Migration Behavior of Carbon Steel Corrosion Products.
Topical Meeting on Nuclear Waste Packaging (FOCUS-91), Las Vegas 1991 (In print)

9 **Nakayama.G. & Akashi,M.**
The Critical Condition for the Initiation of Localized Corrosion of Mild Steels in Contact with Bentonite Used for Nuclear Waste Package.
MRS XV Int. Symp. for Nucl. Waste Management, Strasbourg, 1991

List of SKB reports

Annual Reports

1977-78
TR 121
KBS Technical Reports 1 – 120
Summaries
Stockholm, May 1979

1979
TR 79-28
The KBS Annual Report 1979
KBS Technical Reports 79-01 – 79-27
Summaries
Stockholm, March 1980

1980
TR 80-26
The KBS Annual Report 1980
KBS Technical Reports 80-01 – 80-25
Summaries
Stockholm, March 1981

1981
TR 81-17
The KBS Annual Report 1981
KBS Technical Reports 81-01 – 81-16
Summaries
Stockholm, April 1982

1982
TR 82-28
The KBS Annual Report 1982
KBS Technical Reports 82-01 – 82-27
Summaries
Stockholm, July 1983

1983
TR 83-77
The KBS Annual Report 1983
KBS Technical Reports 83-01 – 83-76
Summaries
Stockholm, June 1984

1984
TR 85-01
Annual Research and Development Report 1984
Including Summaries of Technical Reports Issued during 1984. (Technical Reports 84-01 – 84-19)
Stockholm, June 1985

1985
TR 85-20
Annual Research and Development Report 1985
Including Summaries of Technical Reports Issued during 1985. (Technical Reports 85-01 – 85-19)
Stockholm, May 1986

1986
TR 86-31
SKB Annual Report 1986
Including Summaries of Technical Reports Issued during 1986
Stockholm, May 1987

1987
TR 87-33
SKB Annual Report 1987
Including Summaries of Technical Reports Issued during 1987
Stockholm, May 1988

1988
TR 88-32
SKB Annual Report 1988
Including Summaries of Technical Reports Issued during 1988
Stockholm, May 1989

1989
TR 89-40
SKB Annual Report 1989
Including Summaries of Technical Reports Issued during 1989
Stockholm, May 1990

1990
TR 90-46
SKB Annual Report 1990
Including Summaries of Technical Reports Issued during 1990
Stockholm, May 1991

1991
TR 91-64
SKB Annual Report 1991
Including Summaries of Technical Reports Issued during 1991
Stockholm, April 1992

1992
TR 92-46
SKB Annual Report 1992
Including Summaries of Technical Reports Issued during 1992
Stockholm, May 1993

Technical Reports
List of SKB Technical Reports 1993

TR 93-01
Stress redistribution and void growth in buttwelded canisters for spent nuclear fuel
B L Josefson[1], L Karlsson[2], H-Å Häggblad[2]
[1] Division of Solid Mechanics, Chalmers University of Technology, Göteborg, Sweden
[2] Division of Computer Aided Design, Luleå University of Technology, Luleå, Sweden
February 1993

TR 93-02
Hydrothermal field test with French candidate clay embedding steel heater in the Stripa mine
R Pusch[1], O Karnland[1], A Lajudie[2], J Lechelle[2], A Bouchet[3]
[1] Clay Technology AB, Sweden
[2] CEA, France
[3] Etude Recherche Materiaux (ERM), France
December 1992